High Resolution Seismic Reflection Investigation of the Subsidence Feature on U.S. Highway 50 at Victory Road Near Hutchinson, Kansas

Richard D. Miller

Kansas Geological Survey
1930 Constant Avenue
Lawrence, Kansas 66047

Final Report to

Robert Cook
Kansas Department of Transportation, District 5
Hutchinson, Kansas

Open-file Report No. 2002-17

June 2002

High-Resolution Seismic Reflection Investigation of the Subsidence Feature on U.S. Highway 50 at Victory Road Near Hutchinson, Kansas

Richard D. Miller
Kansas Geological Survey
1930 Constant Avenue
Lawrence, KS 66047

Final Report to

Robert A. Cook
Kansas Department of Transportation, District 5
500 North Hendricks, P.O. Box 769
Hutchinson, Kansas 67504-0769

Open-file Report No. 2002-17 June 2002

High-Resolution Seismic Reflection Investigation Of the Subsidence Feature on U.S. Highway 50 at Victory Road Near Hutchinson, Kansas

Preface

This report has two summaries of this study. The first is an *executive summary* targeting the nontechnical or management reader. The second is a *technical summary* designed for the geoscientist, engineer, or more technically based reader. Information provided in this report is based on data collected at the U.S. 50/Victory Road site and in the collective experience studying dissolution features in Kansas and around the world over the last twenty years. Both insight and methodology developed on non-Kansas funding has provided the lion's share of capabilities used to address this very important and potentially threatening hazard. This report also includes three appendices which include field photographs and printouts of PowerPoint presentations of this study and seismic reflection profiling in general.

Executive Summary

Surface monitoring of a sinkhole at the intersection of U.S. 50 with Victory Road in Reno County began in 1998 when the depression measured about 1 ft below construction grade. Routine elevation surveys conducted since that time have documented average subsidence rates of around 10 inches per year with a cumulative drop in the highway surface of 3 ft since construction. The current sinkhole is centered about 100 ft northwest of the intersection, possesses a very symmetric, 300 ft wide bowl-like shape, and pools water most of the year.

High-resolution seismic reflections mapped the upper 800 ft of earth around and below the sinkhole. The survey consisted of two approximately one-mile seismic reflection profiles that crossed at the intersection of the U.S. highway and county road. The seismic data mapped several key rock layers in the upper 1000 ft and allowed an estimate of surface and subsurface growth potential and rates and the identification of rock layers with structural characteristics that might threaten highway stability. The high signal quality and resolution of these seismic reflection data permitted detection, delineation, and evaluation of all the major rock units associated with the sinkhole.

At this location over the last million or so years groundwater has leached voids in the 400 ft deep, 135 ft thick Permian-aged Hutchinson Salt member of the Wellington Formation. Rocks above the salt have collapsed into these voids. Mechanisms and gross chronology of structural failures interpreted on seismic sections indicate initial subsidence and associated rock failure occurred as accumulated stress on roof rocks spanning salt voids exceeded the strength of roof rock. A chimney-like feature, narrowing upward from its widest point at the top of salt, formed as a result of this roof rock failure. As the initial downward movement (settling, relaxation) of sediments into this chimney feature slowed after formation, gradual subsidence of sediments both within and bounding this chimney feature continued, advancing the surface expansion of the bowl-shaped depression. The rate of destabilization and failure as well as the load-bearing potential of the rock layers above zones of dissolution strongly influence the original subsidence geometries and dimensions as well as the subsequent reactivation of subsidence.

This sinkhole is likely related to the reactivation of natural salt dissolution processes responsible for a 1500 ft wide, sediment-filled paleosinkhole that first formed around a million or so years ago and has since filled with sediments. If salt dissolution has begun again at this site—anthropogenic or natural—it is not possible with these data alone to definitively identify a fluid source or pathway. However, with the position of this modern sinkhole relative to the paleosubsidence feature, and proximity of the nearest disposal well with a history of fluid containment problems, this particular sinkhole is likely the result of natural processes. Besides the obvious disruption to the road system caused by this subsidence, breaching in the confining properties of the bedrock during subsidence might produce a new pathway between the fresh waters of the Equus Beds and the more brackish Permian waters and therefore a threat to water quality.

With a subsidence history at this site potentially extending back over 1 million years, it is unlikely the processes will end within the next millennium. Surface subsidence will likely continue at a gradual rate along the northern and eastern edges of the current sinkhole for some time into the future. Until the highway started sinking at this location sometime before the 1998 elevation survey, little if any subsidence seems to have taken place throughout the last 500,000 years. This long period of inactivity followed by the localized, rapid (3 ft in four years) subsidence recently observed at this site suggests subsurface conditions have changed and the environment is again conducive for leaching and/or failure. It is therefore reasonable to expect similar small sinkholes to form over the next several tens of years above this or other paleofeatures in the area. Sufficient bridging and under-compacted rock layers still exist beneath this sinkhole to sustain the current subsidence rate of around 1 ft/yr for several years to come.

Technical Summary

High-resolution seismic reflections were used to map the upper 800 ft of sediments around and below an actively subsiding sinkhole currently affecting the stability of U.S. 50 highway in Reno County, Kansas. Primary objectives of this study were to delineate the subsurface expression of this growing salt dissolution induced sinkhole and appraise the sinkhole's threat to both highway stability and the highway's characteristically heavy traffic load. The high signal-to-noise ratio and resolution of these seismic reflection data allowed detection, delineation, and evaluation of rock failure and associated episodes of material collapse into voids left after periodic and localized leaching of the 400 ft deep, 125 ft thick Permian Hutchinson Salt member. Mechanisms and gross chronology of structural failures as interpretable from stacked seismic sections suggest initial subsidence and associated bed offset occurred as accumulated stress was rapidly released within a tensional dome defined by reverse fault planes. As the downward movement (settling, relaxation) of sediments slowed with little or no incremental build up of stress, gradual subsidence continued in the subsurface, advancing as an ever-expanding bowl, geometrically defined by normal fault planes.

Several episodes of subsidence are evident in dissolution related features (current and paleo) imaged on these two ¾-mile long seismic profiles. The rate of destabilization and failure as well as the load bearing potential of the rock layers above zones of dissolution are strongly

influenced by both the original subsidence geometries and dimensions as well as the subsequent reactivation of subsidence along the profiles. The sinkhole at the intersection of U.S. 50 and Victory Road is probably related to the reactivation of natural salt dissolution processes that produced the seismically imaged, 1500 ft wide paleosubsidence feature interpreted to have been active during Tertiary and/or Quarternary. Alternately, this current sinkhole could be from delayed failure of overlying Permian rock layers bridging voids or rubble areas in the salt for hundreds of thousands of years following the initial Tertiary to Quaternary subsidence.

Interpretation of reflections from key stratigraphic horizons suggests initial plastic deformation of rock layers over dissolution voids was followed by roof rock failure along reverse fault failure planes within an earth volume known as the tension dome. The original tensional dome was centered on the dissolution volume and extended from the base of the salt interval to near the ground surface. A long period (a significant portion of late Tertiary and early Quaternary) of relaxation of stress associated with layers outside the tensional dome remaining after failure occurred along normal fault planes. A much smaller tensional dome located at the western extreme of the original tensional dome controls recent and current subsidence. Subsidence associated with failure defined by this most recent dome has followed a somewhat asymmetric path from the salt to surface.

With a subsidence history at this site potentially extending as far back as mid-Tertiary, it is unlikely subsidence will end within the next millennium. Until the highway started sinking at this location during or just prior to 1998, little if any subsidence seems to have been associated with this buried sinkhole throughout late Quaternary. This long period of inactivity followed by the localized, rapid subsidence currently observed at this site makes it reasonable to expect other small sinkholes will form without warning above this or other similar paleofeatures in the area. Considering the interpreted bed geometries, slumping of the ground surface at the intersection of Victory Road and U.S. 50 will likely continue gradually along the northern and eastern edges of the seismically defined paleostructure, elongating the sinkhole in those directions. Besides the obvious disruption to the road system, unfortunately this subsidence feature provides a pathway for fresh waters of the Equus Beds to come in contact with the more brackish waters of the Permian, or vice versa. Sufficient bridging and undercompacted rock layers still exist beneath this sinkhole to sustain the current gradual subsidence rate of around 1 ft/yr for several years to come.

If salt dissolution has begun again at this site—anthropogenic or natural—it is not possible with these data alone to confidently identify a fluid source or pathway. However, with the superimposition or juxtaposition of this modern sinkhole and the mid-Tertiary to early Quaternary subsidence feature, and considering the nearest disposal well with a history of fluid containment problems is more than 1.5 miles away, the sinkhole is likely natural in origin. Unfortunately, considering the long history of oil field disposal well-induced dissolution in this area and the proximity of this particular site to the natural dissolution front, neither of these catalysts or fluid sources can be completely ruled out.

Apparent undulations in the surface of the Hutchinson Salt layer could be indicative of dissolution features bridged by undisturbed rock layers with a span not yet sufficient for the accumulated load to instigate roof failure or creep. Roof rock failure above voids associated with excessive leaching of salt can proceed at varying rates and affect different portions of the overlying rock column. These undulations could also be indicative of changes in water chemistry (salinity) during or near the conclusion of salt deposition in this area. An apparent halt in the upward movement of a dissolution feature (downward movement of sediments) at the boundary between the Ninnescah Shale and the Upper Wellington Shale provides insight into the effective unsupported span of roof rock these shallow shale layers can support before failure, and, therefore, the size of the tensional dome to be expected along the dissolution front.

This study also evaluated the effectiveness of using high-resolution vibroseis on the shoulder of U.S. 50 when traffic was slowed but not stopped. Previous data collected in this area was acquired along a quiet, east/west county road 1 mile south of U.S. 50 using a small recording channel seismograph and an invasive, low energy, impulsive source survey. Equivalent dominant frequencies were recorded on both surveys, with the more recent efforts resulting in significantly greater energy penetration and a signal-to-noise ratio sufficient that usable data were recorded regardless of background noise levels. The bed resolution, coherency of bedding within subsidence features, and overall signal-to-noise ratio were greatly improved using minivibroseis survey techniques.

Introduction

Sinkholes are common hazards to property and human safety the world over (Beck et al., 1999). Their formation is generally associated with subsurface subsidence resulting from rock layer failure when overburden load exceeds the strength of the roof rock bridging voids or rubble zones formed by dissolution and/or mining. Understanding sinkhole processes and what controls subsidence rates is key to reducing their impact on human activities, and in the case of anthropogenic, potentially avoiding their formation altogether. Sinkholes can form naturally or anthropogenically from subsidence of rock layers into voids left after the dissolution of limestone (karst), gypsum, or rock salt or from mine/tunnel collapse. With the worldwide abundance of limestone, karst-related sinkholes are by far the most commonly encountered and studied. Both simple and complex sinkholes have formed catastrophically and/or gradually, as the result of dissolution of limestone or rock salt, and by natural and man-induced dissolution processes in many parts of Kansas (Merriam and Mann, 1957).

In central Kansas most sinkholes have formed as the result of the leaching of the Permian Hutchinson Salt member of the Wellington Formation (Watney et al., 1988). Sinkholes forming above regionally continuous salt layers have been studied throughout Kansas (Frye, 1950; Walters, 1978) and the United States (Ege, 1984). Studies based on surface and/or borehole observations of subsidence over the Hutchinson Salt in Kansas has focused on mining around Hutchinson, Kansas (Walters, 1980), disposal of oil field brine near Russell, Kansas (Walters, 1991), and natural salt dissolution through fault/fracture-induced permeability (Frye and Schoff, 1942) have drawn conclusions about the mechanism responsible for subsidence geometries and rates. Using only surface observations and borehole data, a large number of assumptions and a good deal of geologic/mechanical sense must be drawn on to define and explain these features and their impact. High-resolution seismic reflection profiling has proven an effective tool in mapping the subsurface expression and predicting future surface deformation associated with dissolution of the Hutchinson Salt in Kansas (Steeples et al., 1986; Miller et al., 1993; Anderson et al., 1995a; Miller et al., 1995; Miller et al., 1997).

Salt dissolution sinkholes are found in all areas of Kansas where the Hutchinson Salt is present in the subsurface (Figure 1). Stem pressure tests and/or seismic reflection investigations have definitely correlated sinkholes to containment failure in disposal wells (injecting oil field brine wastewater) at a variety of sites throughout central Kansas (Steeples et al., 1986; Knapp et al., 1989; Miller et al., 1995; Miller et al., 1997). Sinkholes which have formed by natural dissolution of the Hutchinson Salt and resulting subsidence processes are most commonly documented along the depositional edges on the west and north and the erosional boundary on the east (Frye and Schoff, 1942; Frye, 1950; Merriam and Mann, 1957; Anderson et al., 1995a). The vast majority of published works studying the source of localized leaching of salt in Kansas directly contradict suggestions that recent land subsidence in Kansas is mostly natural in origin (Anderson et al., 1995a).

Natural dissolution of the Hutchinson Salt is not uncommon in Kansas and has been occurring for millions of years (Ege, 1984). Faults extending up to Pleistocene sediments containing fresh water under hydrostatic pressure are postulated as the conduits instigating salt dissolution and subsidence along the western boundary of the salt in Kansas (Frye and Schoff, 1942). Paleosinkholes resulting from dissolution of the salt prior to Pleistocene deposition have been discovered with high-resolution seismic surveys (Miller et al., 1985; Anderson et al., 1998).

Seismic reflection data targeting beds altered by dissolution and subsidence in this area have ranged in quality and interpretability from poor (Miller et al., 1995) to outstanding (Miller et al., 1997). Interpretations when data quality is poor (i.e., low signal-to-noise ratios) have unfortunately been relegated to indirect inference of structural processes and subsurface expression through interpretations of structural deformation in layers above the salt. However, data with excellent signal-to-noise ratios and resolution have allowed direct detection of structures and geometries that appear characteristic of complex sinkholes. Resolution potential and signal-to-noise ratio of seismic data from this study are superior to any previously published targeting the salt interval in Kansas. These data provide conclusive images of important structural features and unique characteristics that control sinkhole development.

Subsidence of U.S. 50 below construction grade at its intersection with Victory Road totaled 1 ft when first measured during a 1998 elevation survey. Routine elevation surveys conducted since that time have monitored the pattern and rate of subsidence. At an average subsidence rate of around ¾ ft/yr, the highway surface at its centerline has sunk about 3 ft since construction. The current sinkhole is symmetric, with a very regular bowl-shaped geometry around 300 ft in diameter retaining water most of the year.

The sinkhole is centered a hundred feet or so to the northwest of the intersection of U.S. 50 and Victory Road (Figure 1). The symmetry and compact nature of the sinkhole as well as it subsidence rate is consistent with conceptual models of sinkhole formation when salt is leached by borehole-released fluids (Walters, 1978; Miller et al., 1997). These similarities in geometry and subsidence rates raise suspicions that this feature might somehow be related to oilfield waste water disposal even though no records or surface installations exist supporting that suggestion. Two seismic reflection profiles acquired orthogonally to each other and centered on the intersection of the highway and county road provided optimal coverage for mapping bed geometries, growth potential, and future surface footprint associated with this sinkhole and for identifying structural characteristics that might someday put vehicle traffic at risk.

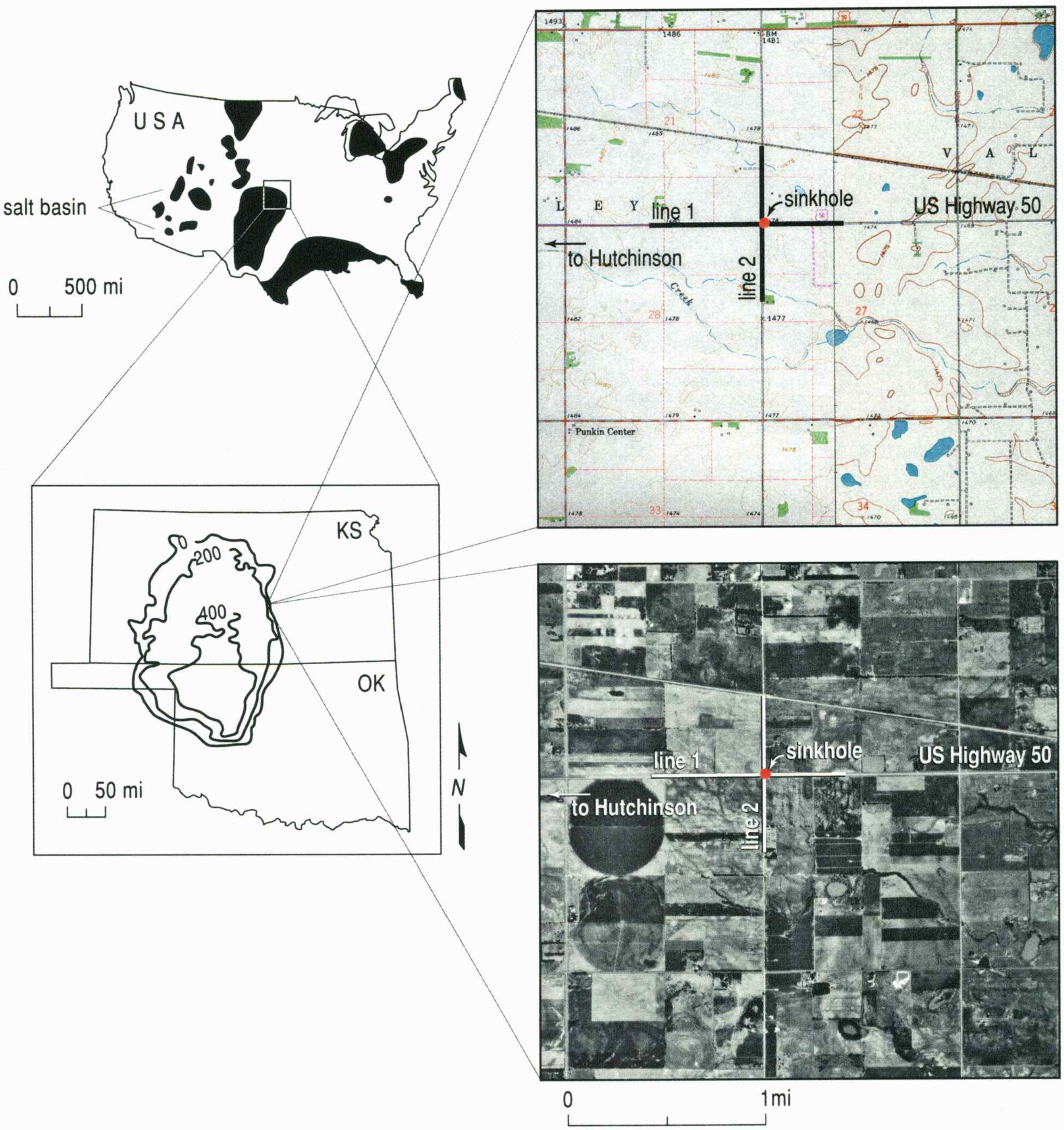

Figure 1. Site map relative to bedded salt deposits (from Ege, 1984). The Hutchinson Salt is a bedded salt deposit extending from central Oklahoma across most of south-central Kansas (Walter, 1978). Along the eastern extreme of the salt bed is the currently active dissolution front responsible for many natural dissolution features, both sinkholes and paleosubsidence. Two 1-mile seismic profiles tie at the intersection of U.S. Highway 50 and Victory Road in Reno County, Kansas.

Geologic Setting

Several major salt basins exist throughout North America (Ege, 1984). The Hutchinson Salt Member occurs in central Kansas, northwestern Oklahoma, and the northeastern portion of the Texas panhandle, and is prone to and has an extensive history of dissolution and formation of sinkholes (Figure 1). In Kansas, the Hutchinson Salt possesses an average net thickness of 250 ft and reaches a maximum of over 500 ft in the southern part of the basin. Deposition occurring during fluctuating sea levels produced numerous halite layers, 0.5 to 10 ft thick, interbedded with shale, minor anhydrite, and dolomite/magnesite. Individual salt beds may be continuous for only a few miles despite the remarkable lateral continuity of the salt as a whole (Walters, 1978).

The eastern margin of the salt was exposed during late Tertiary where erosion and leaching began the dissolution front's 10-mile westward progression to its present day location (Bayne, 1956). The ability of the front to migrate while under as much as 300 ft of sediments is a direct consequence of the ready access to an abundant supply of groundwater (Watney et al., 1988). Subsidence of Permian, Cretaceous, Tertiary, and Quaternary rocks has progressed along the migration front as the salt has been leached away. During and after this subsidence, Quarternary alluvium was deposited in volumes consistent with the depressed surface topography sculpted as the salt was being removed. This process has resulted in today's moderate to low surface relief topography that masks the extremely distorted (faulted and folded—non-tectonic) rock layers within the upper Wellington and Ninnescah shales (Anderson et al., 1998). Around 100 ft of salt is still in place at the U.S. 50/Victory Road site where a maximum of around 275 to 350 ft once existed.

Permian redbed evaporites overlaying the Hutchinson Salt Member are a primary target of any study focusing on salt dissolution induced sinkhole development and associated risks to the environment and human activity in Kansas. Failure and subsidence of these evaporite units are a factor in the eventual formation of sinkholes, but more importantly, once the natural confining characteristic of these rock layers has been compromised, a pathway is established for groundwater mixing (fresh and brackish) and access by these waters to the salt. Fractures, faults, and collapse structures in proximity to the dissolution front compromise the confining properties of the Permian shale bedrock and put the major fresh water aquifer (Plio-Pleistocene Equus Beds) in this part of southern Kansas at risk. Along the eastern boundary (dissolution front) the salt, which ranges from 0 to over 300 ft thick, is buried beneath about 400 ft of Permian redbed evaporites and Cenozoic sediments.

Rock salt under a depositional load is almost incompressible, highly ductile, and easily deformed by creep (Baar, 1977). Plastic deformation of the salt associated with creep is expected naturally to occur in these salts (Anderson et al., 1995b). Thin anhydrite beds within the halite succession have a strong acoustic response and therefore are seismically imageable and can provide a measure of mechanical deformation within the salt interval. Considering the extreme range of possible strain rates the salt can experience during creep deformation, these thin interbeds can possess quite dramatic geometries, especially high amplitude, short wavelength folding.

Dissolution-Induced Subsidence

Subsidence can occur at rates ranging from gradual to catastrophic, continuous to segmented. Subsidence rates to some extent relate to the type of deformation in the salt (ductile or brittle), the strength of rocks immediately above the salt layer, and the depth to the top of salt. As salt is leached, pore space is created. As this pore space grows it eventually gets large enough to provide the differential pressure necessary to support creep (Carter and Hansen, 1983). If this pore space continues to grow it can attain a size that exceeds the strength of the roof rock, the unsupported span will fail, and subsidence occurs. Strength of the roof rock and size of the void dictate rock failure characteristics within and just above the salt, and therefore control how the void progresses upward. In general, gradual surface subsidence is associated with ductile deformation accommodating both vertical and outward growth of the sinkhole, forming an ever-enlarging bowl-shaped depression with bed geometries and offsets constrained by normal fault geometries (Steeples et al., 1986; Anderson et al., 1995b). When rapid to catastrophic subsidence rates are observed, failure within the salt is usually brittle with the void area migrating to surface as an ever-narrowing cone defined by bed offsets and rock failure controlled by reverse-type fault planes (Davies, 1951; Walters 1980; Rokar and Staudtmeister, 1985).

Lithostatic load is the key to the development of breakdown and associated subsidence (Davies, 1951). Before a cavern forms, the vertical and horizontal components of stress acting at any point in the subsurface are in equilibrium. When an opening forms, these forces are no longer in equilibrium and a new stress regime develops which is strongly dependent on the strength of the roof rock and overburden. Once the strength of the roof rock is overcome, the roof and/or walls are forced into the opening. Vertical stresses cause beds in the overburden to drape (sag) and separate at physical contacts above the cavern. The extent of this separation and sag is a function of material strength and cavity dimensions and is represented in three dimensions by a tension dome (Figure 2). Assuming horizontal beds above the cavity or void are of similar physical strength, sag is greatest around a vertical axis centered on the opening (or cavity) lessening upwards with decreasing depths. After bed separation, lithostatic load cannot be transmitted within the tension dome, and stress is transferred to rocks along the dome boundary and the walls of the cavity. Rock outside the tension dome has no direct impact on the mechanics of

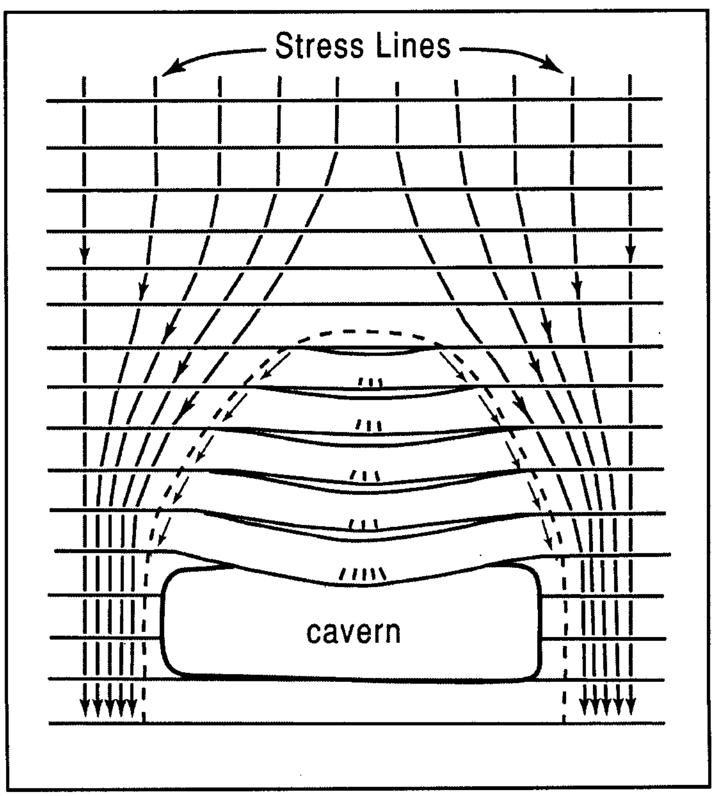

Figure 2. Tension dome and distribution of stress lines around a cavern opening in horizontal strata (Davies, 1951).

breakdown. It is the weight and physical properties of the rock units within the dome that cause and control collapse. Failure generally occurs first on sagging roof rock close to the wall where shear forces are the greatest.

Collapse of rocks within the tension dome begins once layer sag reaches the point of failure. Depending on the rock properties and void specifics, collapse can be confined to the lowermost unit that forms the ceiling of the void or massive breakdown can occur if successive beds fail within the dome. In the latter, it is possible for failure to start in many different locations within the dome. Depending on material properties and stress levels, the lowest bed may collapse, progressing gradually upward into the overlying units, or collapse can be initiated by failure of any unit within the dome. Most breakdowns can be attributed to the latter mechanism where a sagging bed within the dome fails rapidly, transferring its weight to the bed below. Failure of underlying units follows much like dominos due to the increased load. Such a sequence of failures extends over a considerable vertical distance and typically culminates in roof collapse. Failure of intermediate layers within the dome is a plausible mechanism for catastrophic subsidence rates observed in select sinkholes throughout central Kansas.

For sinkholes to form catastrophically, the pre-failure stress field as defined by the tensional dome must include all rock units between the void and ground surface. Since rocks outside the tension dome have no direct impact on the mechanics of breakdown, earth materials affected by void-induced collapse are limited to the volume within the tensional dome at the time of failure. As well, once a void grows large enough to instigate roof rock failure, the main factors controlling the speed rock collapse moves upward toward the ground surface is the distance between the top of the tensional dome and ground surface and the physical properties of the rocks within the tensional dome. Once failure commences, a sinkhole will form as a somewhat continuous and rapid event if the tensional dome extends to the ground surface. Surface facilities or human activity are only at risk if they are within the tensional dome. Within 5 miles of this sinkhole catastrophic surface failure associated with overmining of salt has been observed and seismically studied (Miller et al., 1993). Something to be considered: Since the tensional dome is an area with elevated stress such that the stress/strain relationship as defined by Young's Modulus could become nonlinear just prior to failure, subsidence risk should be quantifiable through study of lateral variations in the shear wave velocity field. Development of an early warning system might be possible.

Subsidence rates are difficult to predict and deformation sequences associated with subsidence are generally complex. Dissolution of the Hutchinson Salt and the resulting subsidence has been suggested to form through reverse faulting extending from the salt voids to the surface (Walters, 1978). High-resolution seismic reflection surveys during the later half of the twentieth century were only been able to conclusively map normal faults stepping away from the salt void as they extend to the surface (Steeples et al., 1986; Miller et al., 1995). Data from a study in the late 1990s at a brine disposal well-induced sinkhole in central Kansas was the first to conclusively identify reverse faulting present at the boundaries of the tensional dome defining the volume affected by initial roof rock failure on seismic data (Miller et al., 1997). This initial failure was then followed by a period of relaxation characterized by a sequence of normal faults interpreted in rock layers above the salt. These normal fault oriented ruptures begin outside the tensional dome and step away from the edge of the dissolution zone in general to form a synform. Considering the very fluid nature of layered salt deposits as the salt is squeezed and moves into void areas, overlying rocks will sag and stabilize this high-energy environment. Both reverse and normal faulting are associated with the subsidence process above dissolution voids in the Hutchinson Salt.

Seismic Acquisition

The seismic survey was designed to include two seismic lines, each possessing at least ¾ mile of full-fold subsurface coverage centered on the sinkhole. This design insured a clear and complete image of the entire subsurface "root" of the sinkhole was obtainable. With the sinkhole conveniently located at the intersection of U.S. 50 and Victory Road, the two seismic lines were acquired orthogonal to each other and along the roads where surface materials and coupling were relatively consistent. This design provided the best fold and azimuthal coverage throughout the Permian section. To eliminate the need for a roll-along switch and extend the range of far offsets available to choose from during processing a rolling fixed-spread design was used to record these data (Figure 3). This survey configuration provided the wide range of source offsets necessary for detailed velocity analysis and minimized wavelet distortion, a close receiver spacing for improved confidence in event identification, and maximized the range of imageable depths.

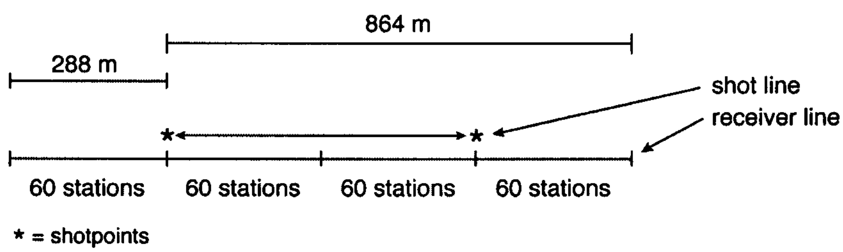

Figure 3. Fixed 240-channel spread with shooting geometry for asymmetric split spread.

The modern sinkhole is a subdued, miniaturized expression of the subterranean rock layers disturbed by Tertiary or older salt dissolution and the resulting million years plus of subsidence. Based on seismic reflection surveys, all sinkholes in Kansas formed from the leaching of salt possess an effective subsurface "root" or disturbed volume with at least twice the cross-sectional area as the sinkhole itself. To avoid shortfalls in subsurface coverage as experienced in some previous seismic investigations of Kansas sinkholes, this survey was designed to high-fold sample a 2-D subsurface slice ten times the current diameter of the sinkhole.

Acquisition parameters were defined based on experience gained during previous surveys and walkaway tests along line 1. Twin Mark Products L28E 40Hz geophones were planted at 8 ft intervals in approximate 2 ft arrays (Figure 4). Geophones were planted into firm to hard soil at the base of the road ditch in small divots left after the top few inches of loose material were removed to insure good coupling (Figure 5). Four 60-channel Geometrics StrataView seismographs were networked to simultaneously record 240 channels of data (Figure 6). An IVI Minivib using a prototype Atlas valve delivered three 10 second, 25-250 Hz up-sweeps at each shot location spaced 16 ft apart (Figure 7). Experiments at this site were consistent with bench tests, suggesting this new rotary valve design produces up to four times the peak force of conventional valves at 250 Hz (Figure 8). The pilot was telemetried from the vibrator to the seismograph and

Figure 4. Two Mark Products L28E 40 Hz geophones separated by about 1 ft to form a 2 ft effective array.

Figure 5. Receivers were "planted" at the base of the road ditch to insure highest possible quality coupling.

Figure 6. 240 channel Geometrics StrataView with support electronics (line checker, IVI source synchronizer, time break conditioner, etc.).

Figure 7. IVI minivib with Atlas rotary valve. Approximately 800 ft-lbs of force can be applied at 100 Hz, while around 2000 ft-lbs are possible in some conditions at 250 Hz.

Figure 8. 300 lb mass and 300 lb baseplate with new prototype Atlas rotary valve.

recorded as the first trace of each shot record. Each of the three sweeps generated at each shot station was individually recorded and stored with the ground force pilot in an uncorrelated format.

All sweeps were recorded by the fixed 240-channel spread while incrementally moving the source from shot station to shot station through the middle half of the spread after each set of three sweeps was completed (Figure 3). Once the center 120 receiver stations (60 shot stations) were "rolled" through, the back 120 receiver stations were moved to the front and the process repeated. Since all shot records were recorded uncorrelated, QC involved visual inspection of the recorded pilot trace, audio monitoring of the pilot trace on a RF scanner, inspection of the vibrator power spectra after each shot, and review of correlated shot records after every 5 to 10 shot stations. With the exception of receiver stations not instrumented due to gravel or asphalt roads, the survey was recorded with 98 percent live receivers within the optimum recording window (Hunter et al., 1984).

Reflections can be interpreted on raw, correlated shot records (scaled for display purposes) from around 30 ms to two-way time depths in excess of 500 ms (Figure 9). Considering the optimum window these data possess, it was imperative to keep a wide range of offsets to insure imaging of the entire target zone. Reflections with upper corner frequencies of around 200 Hz can be interpreted as deep as 200 ms on stacked sections, while reflections from 500 ms have dominant frequencies that drop to around 100 Hz. Several milliseconds of reflection "chatter" observable between traces in proximity of the sinkhole is

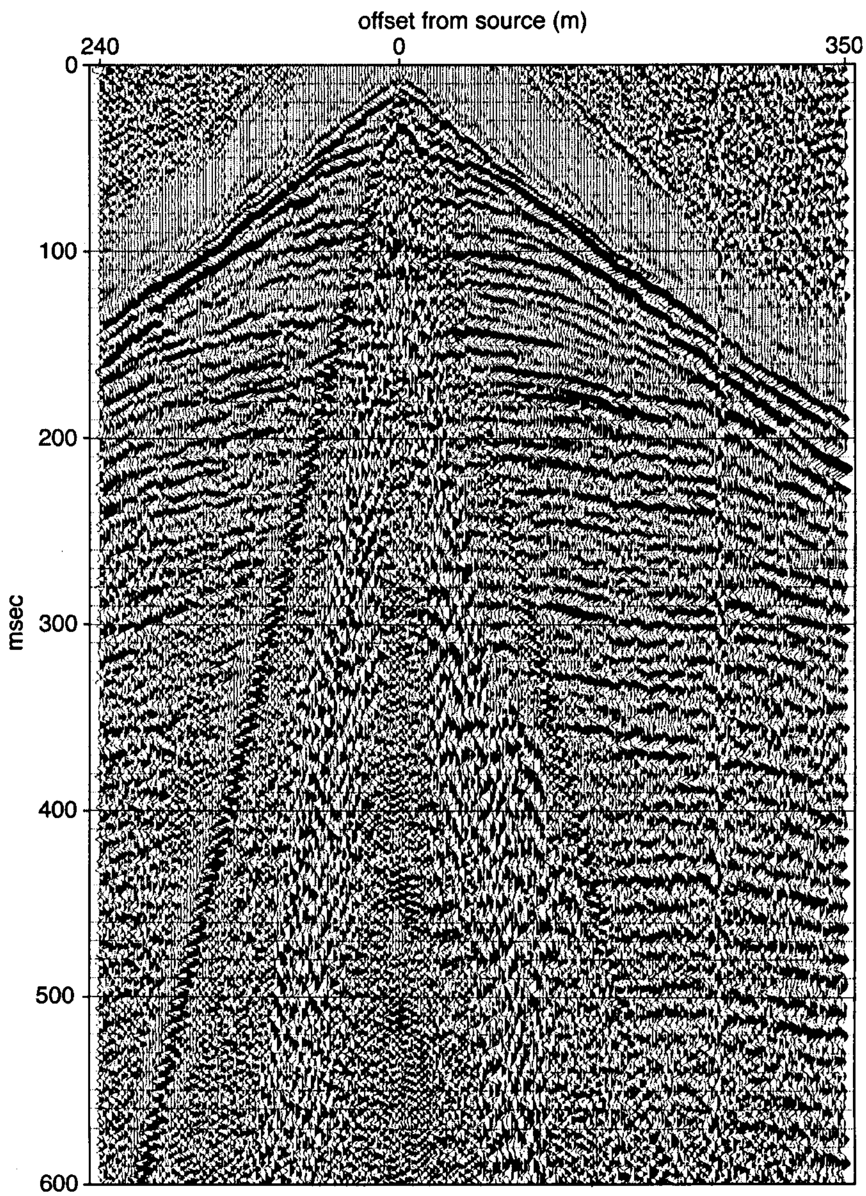

Figure 9. Representative 240-channel shot gather with 2.5 m receiver spacing and IVI minivib source, scaled for display. Dozens of reflections are interpretable in the upper 600 ms. Top of salt is indicated by the high amplitude reflection at about 130 msec.

indicative of the dramatic localized changes in material velocities associated with rock layer failure and subsidence. Considering the dominant frequency of some reflections exceeds 200 Hz, a 2.5 ms static between adjacent traces represents a 180° phase shift and complete cancellation would result if proper adjustments are not made. Therefore, it is critical that these static irregularities be compensated before the data are CMP stacked.

Seismic Processing

The basic CMP processing flow was consistent with 2-D high-resolution seismic reflection methodologies (Steeples and Miller, 1990) (Figure 10). All lines were processed using WinSeis 2, beta seismic data processing software (next generation of WinSeis Turbo, a commercial computer software developed at the Kansas Geological Survey). It is common knowledge that reflection data acquired in highly disturbed subsurface settings, such as near sinkholes and dissolution features, will be plagued with static problems and subject to dramatic swings in NMO velocity over relatively short distances; this data set was no exception. For purposes of this survey the surface topography was considered flat with the exception of the 3 ft deep depression associated with the 300 ft wide sinkhole. Changes in velocity related to differentially compacted fill, anomalous rubble zones, and distorted rock layers produced several millisecond fluctuations in event arrival times across distances as small as 20 to 30 ft (Figure 11). In extreme cases shifts of 10 ms can be measured across a span of less than 30 ft.

Data were recorded and stored uncorrelated to allow application of precorrelation processes designed to increase the signal-to-noise ratio and resolution potential (Doll and Çoruh, 1995). Removal of noisy traces and amplitude balancing were precorrelation processing steps that significantly enhanced signal-to-noise and resolution potential. Attempts to improve the precorrelation data quality through frequency filtering, spectral whitening, and frequency-wave number (F-k) filtering were unsuccessful. Storing data uncorrelated also allowed the downstream testing of different correlation methods and correlating to different pilot traces. Testing verified these data were optimally correlated using the synthetic drive signal. Storing data uncorrelated and unstacked required 30 times more storage space, about 50 percent more acquisition time, and 5 times more data transfer time. Improvements in signal-to-noise ratio and resolution made these increases cost effective.

Emphasis was placed on noise suppression, maintaining true amplitude, and compensating for lateral velocity irregularities. Noise suppression focused on vehicle noise from the highway, livestock in pastures along the seismic lines, powerline noise, surface waves, first arrivals, and air-coupled waves. Muting and hum filtering (Xia and Miller, 2000) improved signal-to-noise appreciably. The three individual shot gathers acquired at each shotpoint were vertically stacked after completing trace-specific noise suppression. With the exception of the 1 sec precorrelation AGC and display gains, only spherical divergence was used to adjust trace amplitudes. With the large depth window of interest, a relatively wide optimum offset window was maintained, which after noise reduction resulted in true CMP trace folds ranging from 1 to a maximum of 30 (Liberty and Knoll, 1998). Velocity was defined for each group of 20 CMPs with five points in the first 200 ms and a minimum of one control point for each subsequent 100 ms time window. Each seismic line has a velocity function containing over 400 time/velocity pairs determined using an iterative approach to correlation static corrections and velocity analysis.

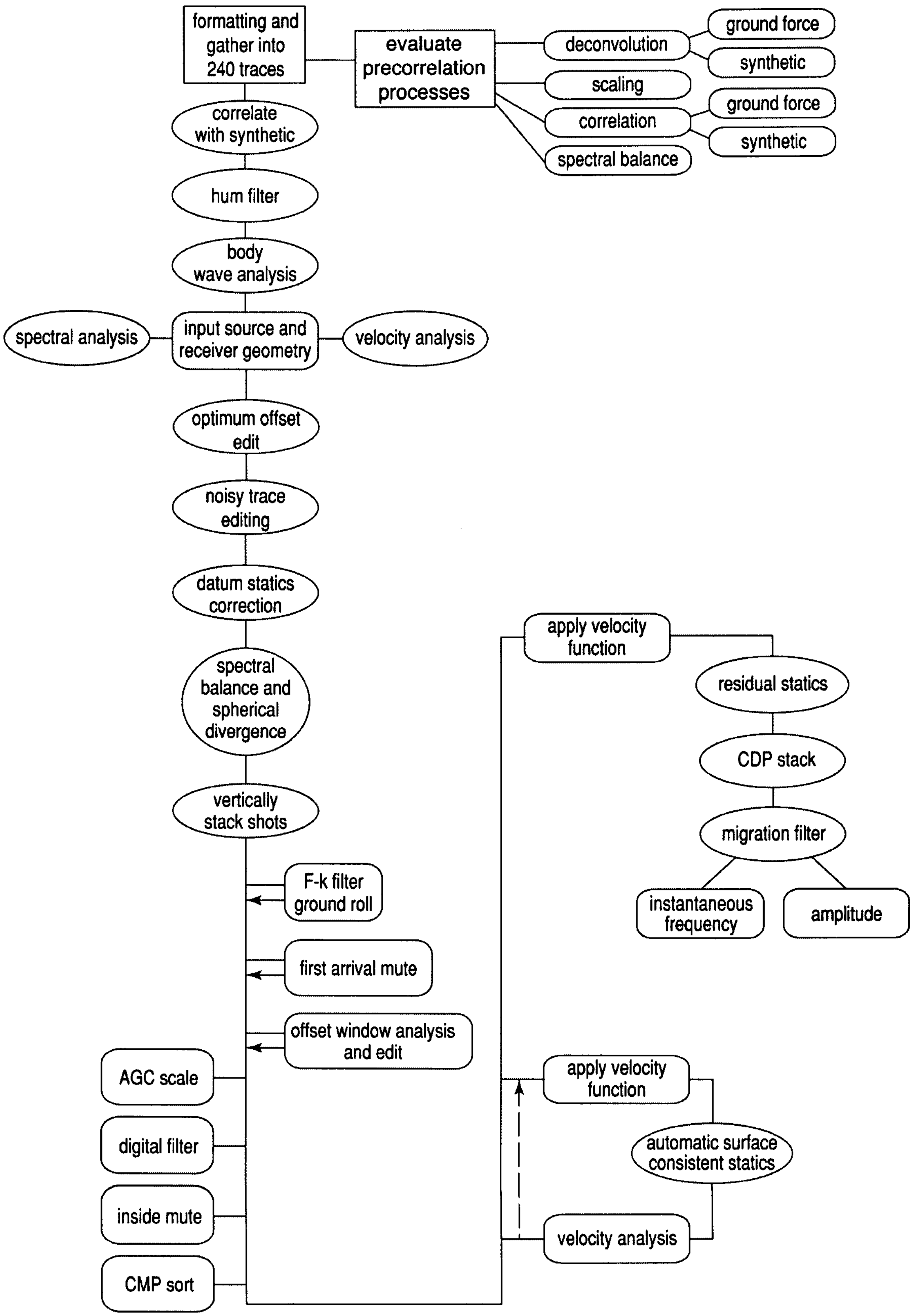

Figure 10. CMP processing flow using WinSeis 2.

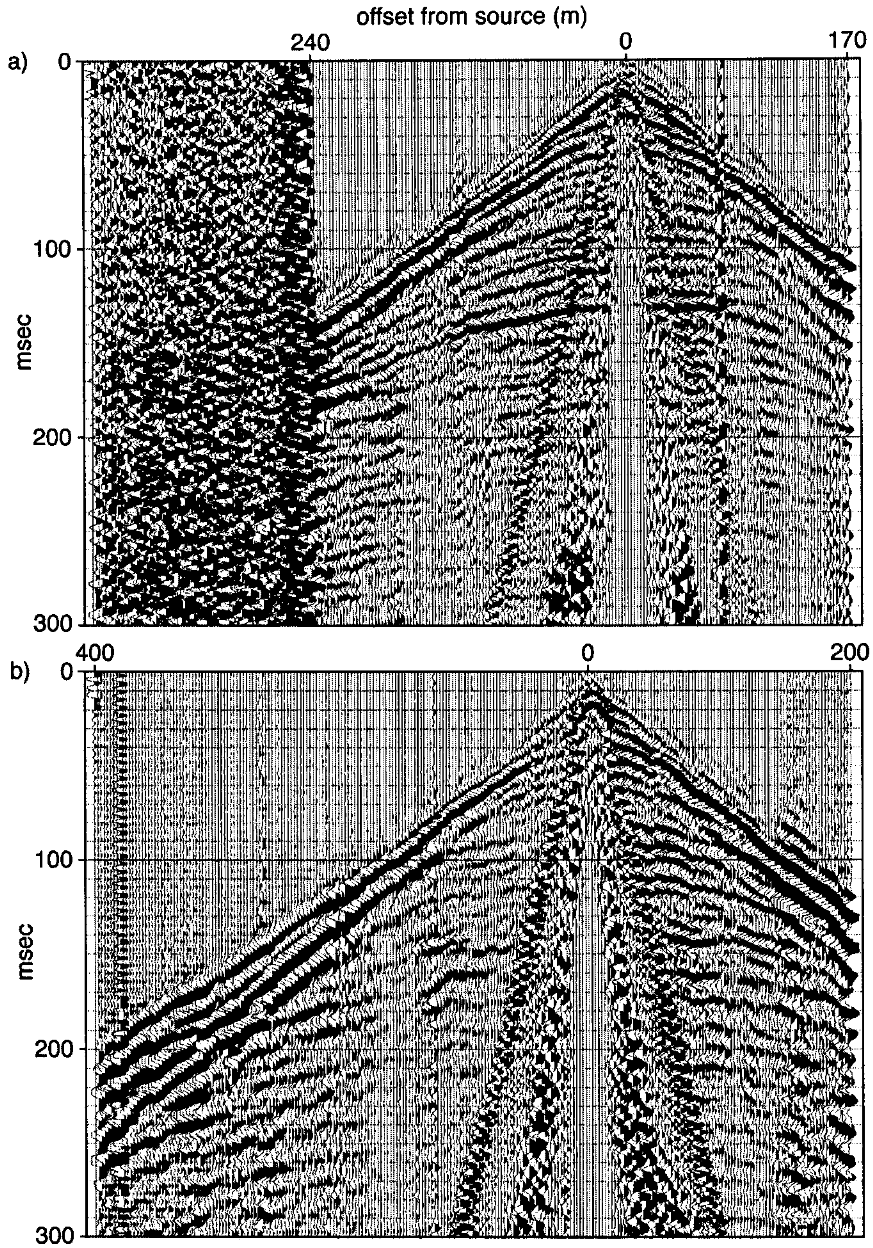

Figure 11. True amplitude shot gathers (24 dB/sec spherical divergence correction) demonstrate the highly variable reflection waveforms which do not seem to correlate to a single change in physical or seismic characteristics (velocity, attenuation, offset, or density), but more likely some complex combination of several. Apparent anisotropic characteristics (in this case attenuation) pronounced on some shot gathers (b), are directly related to the near-surface in close proximity to the source.

Even where reflections were interpretable within the noise cone an inside mute was applied to remove all energy after the air-coupled wave, thereby avoiding signal degradation on CMP stacked sections (Figure 11a). Inside mutes are common practice for shallow (upper 3000 ft) seismic reflection processing (Baker et al., 1998) and only in rare situations does reflection energy emerge from within the surface wave energy packet at high enough amplitudes to warrant foregoing the inside mute. It is however, uncommon and counterintuitive to remove confidently identifiable reflection events regardless of where they are relative to other energy arrivals, but in many cases it is necessary to optimize wavelet attributes. Surgical muting of noise immersed in signal significantly increases the likelihood of reducing the resolution potential or losing some trace-to-trace coherency of reflections through wavelet distortion during stacking. Analogous to inoperable tumors, attempts to precisely remove just noise, especially air-wave noise, at tolerances of a millisecond or two runs the risk of cutting too severely and/or defining mute tapers that are too steep, thereby irreparably altering the reflection waveform and distorting the information it possesses. Stacking waveforms distorted by overly aggressive mutes will compromise the accuracy of the information contained in the waveform, and in some cases produce artifacts that can be misinterpreted as true earth response.

Powerline noise was pronounced on shot gathers along line 2 (Victory Road) (Figure 1). A complex combination of 60 Hz noise and its harmonics (120 Hz and 180 Hz) bled onto cables from overhead power lines running parallel to Victory Road, thereby masking most of the seismic energy even after correlation along portions of the road. A hum filter proved to be very effective in eliminating powerline noise without affecting the amplitude or phase of the seismic data (Xia and Miller, 2000). This predictive filtering approach produced a noticeable increase in signal-to-noise without loss of resolving potential.

Seismic Interpretation

Shot and CMP Gathers

Confidently interpretable reflections on shot gathers are essential to optimizing the acquisition, processing, and interpretation of high-resolution seismic reflection data. Dozens of high-resolution reflections dominate the average shot gather from this site (Figure 11). Reflections throughout the primary target time window (50 ms to 200 ms) possess broad bandwidths and sufficient coherency to clearly interpret their arrivals across several to tens of traces. The irregular chevron-looking (zig-zag) pattern evident in reflections across distances of several traces in and around the sinkhole is related to lateral velocity irregularities and designated as static during processing. The non-linear pattern observed in first arrivals is also the result of velocity irregularities, either at or very near the bedrock surface or between bedrock and the ground surface. Reflection events can be traced through the air-coupled wave and into the ground roll wedge (Figures 11 and 12). To avoid any contamination by source-generated noise (refractions, direct wave, air-coupled wave or surface wave), all energy before the third zero crossing of the first arrival and after the onset of air wave arrival was removed during processing.

For quality control reasons it is important that reflections interpreted at two-way times less than 30 ms on CMP stacks be correlated with equivalent reflection hyperbolae with a 30 ms zero offset time on shot gathers. This consistency between the 30 ms reflection on shot records and stacked sections is evident at various places along both lines of this survey (Figure 12a). Identification of these ultra-shallow reflections on field files and tracking of them throughout the processing flow was necessary to ensure the correctness of timing (geologic) of subsidence as interpreted on CMP sections. These ultra-shallow reflections (< 30 ms) were critical to discerning subsidence activity post-Permian in the sediment-filled paleosinkholes. Besides the reflection "chatter" indicative of lateral variations in material velocity, a striking characteristic of these seismic data is the inconsistent AVO effects that seem most sensitive to source and receiver orientation (Figure 11b). Changes in reflection amplitude in this setting could be indicative of changes in acoustic impedance of the reflector itself and/or lateral variations in attenuation due to rock failure and collapse. True amplitude analysis intended to search for localized changes in material properties, possibly indicative of increased loading, does not seem to be an effective first-order tool. Ineffectiveness of AVO analysis is likely related to extreme attenuation characteristics within the sinkhole that seemed to vary dramatically without a single clear dependency.

Asymmetry of reflection hyperbolae observed on shot gathers across both lines is the result of dipping layers and velocity variability (Figure 12). Apparent shifts in the apex of the reflection hyperbola are likely related to changes in velocity rather than dipping rock units when

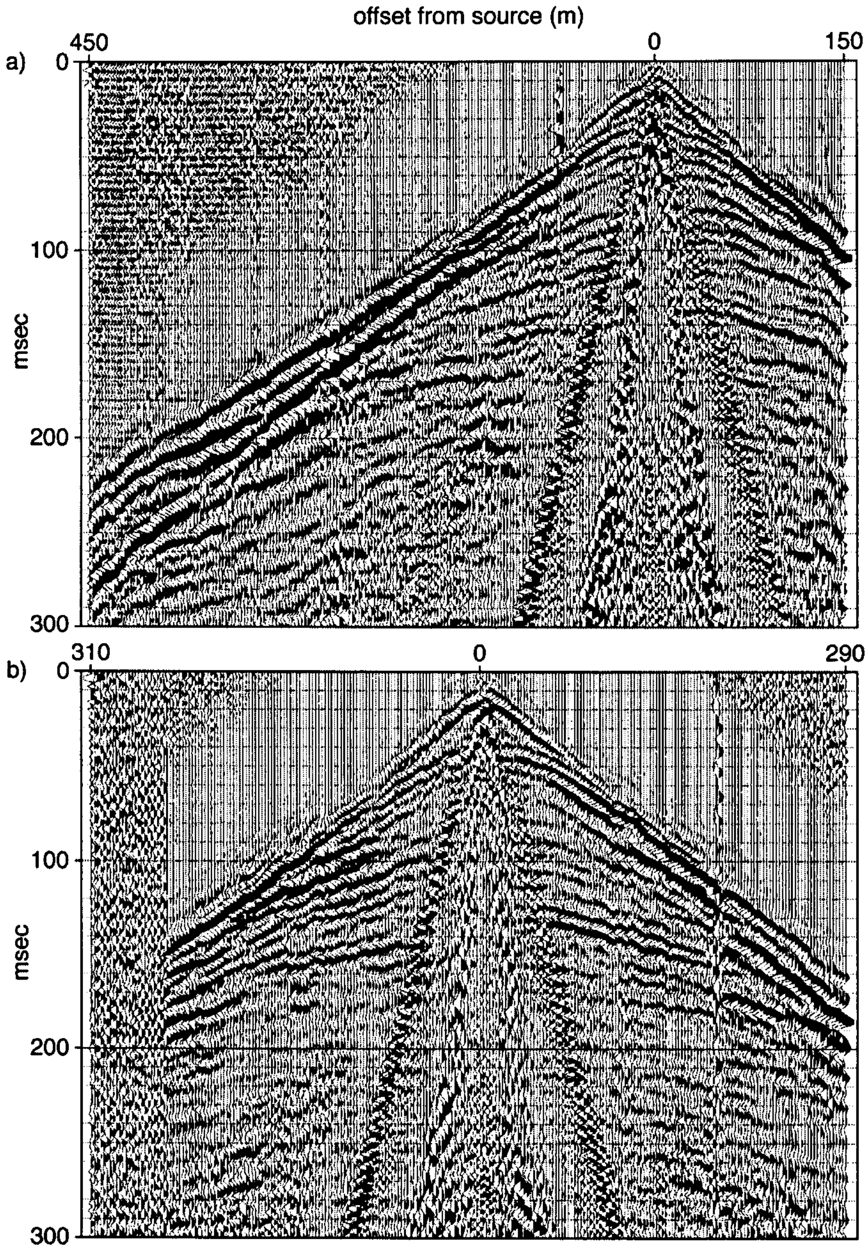

Figure 12. Reflections on shot gathers at two-way times less than 30 ms need to be identified on shot gathers and followed throughout processing (a). Characteristics of shot gather allow confident determinations of where the subsurface has been disturbed (b). Right half of shot gather is outside the rim of the subsurface disturbed zone and the left half is inside. The same reflecting horizon arrives a full 10 ms earlier from one direction than the other.

considering the scale of the distorted rock units relative to the spread length (Figure 12a). Distortions of this kind inhibits NMO velocity corrections based on the juxtaposition of first order theoretical reflection hyperbolae with the moveout of actual reflections on CMP gathers. Many times these kinds of velocity irregularities are "removed" during processing by brute force adjustments using correlation statics techniques after a best fit NMO correction has been made. These kinds of NMO curve perturbations can also result in decreased fidelity and distortion of attributes if not compensated for prior to CMP stacking.

High-resolution delineation of bed offset is often easier and more accurate on shot gathers than CMP stacked sections (Figure 12b). In the CMP domain this offset is observed between adjacent CMPs, where it is evident between traces on shot gathers. Faults that appear abrupt and definable within a few traces on shot gathers can appear smeared across several traces on CMP stacked sections, inhibiting interpretations that maximize the horizontal resolution potential of data. In some places reflections from the top of salt experience 15 ms of difference at equivalent source offsets (less than 100 ft) on opposite sides of the source. Interpreting such fine structural and stratigraphic detail mandates minimal and optimum fold and offset stacked CMP sections.

CMP gathers hold the key to accurate representations of the subsurface from CMP stacked sections. After adjusting reflections for non-vertical incidence, lateral variations in material velocity, and spherical attenuation of energy, they possess broad amplitude spectra and consistent wavelets across the entire optimum offset range (Figure 13). The offset-dependent nature of frequency and amplitude characteristics are most evident in reflections deeper than 100 ms (~300 ft). NMO velocities were defined for the primary reflecting interfaces to insure minimum decay in wavelet frequencies after stacking.

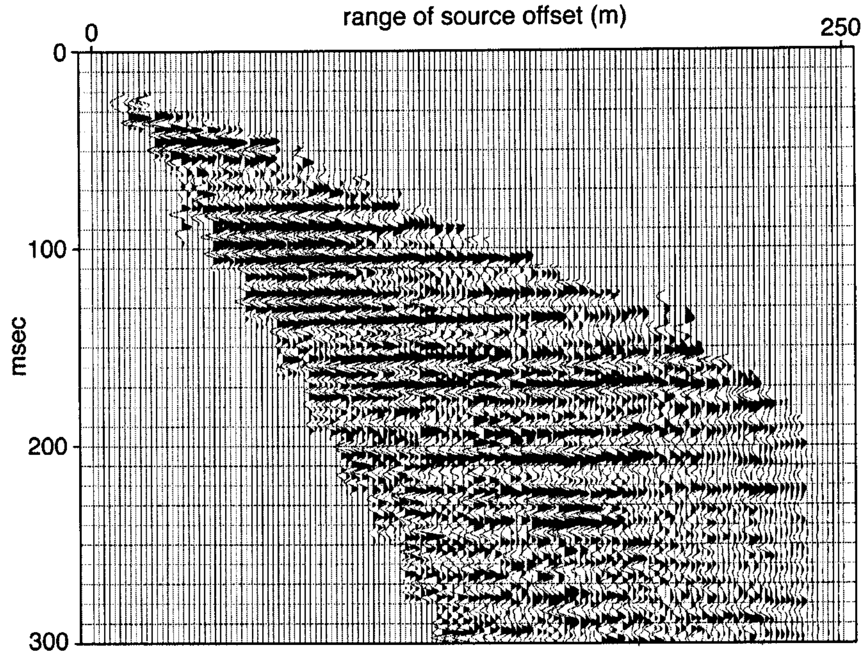

Figure 13. Fully processed CMP gather displaying character of the reflection wavelets just before stacking. Even though there are 120 traces that comprise this CMP, this gather includes each of the three sweeps taken per station, which would equate to a maximum of 40 fold. With the mutes that have been applied, this maximum of 40 fold drops to around 20 fold for any one single reflection horizon on the stacked section.

Seismic Stratigraphy

Seismically all the Permian and younger reflectors provide important clues to accurately replaying and interpreting the subsidence history of this site from stacked sections. Model studies show that significant time delays (static) and geometric distortions below subsidence features are to be expected on vertically incident seismic data (Anderson et al., 1995b) (Figure 14). Static delays or "pull downs" in time result from localized decreases in material velocities within a sinkhole due to changes in compaction and material properties. The velocity structure and small radius of curvature of the synforms, characteristic of salt dissolution and subsidence in this area, generally produce diffractions and distorted reflection arrivals on vertically incident stacked sections. As suggested by modeling, reflections from beneath the salt will have a subdued expression of the subsidence geometry. Estimations of layer subsidence and therefore volume of rock salt removed based on time section estimations alone (without compensation for velocity variability) can exceed actual by as much as 50 percent in this area. In this geologic setting, it is reasonable to compensate for compaction-related static by "flattening" on the top of the Chase Group. However, greater accuracy is obtained through time-to-depth conversion using a tightly defined and realistic velocity function.

Most of the upper 2500 ft of rock at this site is Permian shales (Merriam, 1963). The currently disputed Permian/ Pennsylvanian boundary is about 2500 ft deep and seismically indicated by a strong sequence of cyclic reflecting events. The Chase Group (top at 800 ft deep), Lower Wellington Shales (top at 600 ft deep), Hutchinson Salt (top at 400 ft deep), Upper Wellington

Shales (top at 225 ft deep), and Ninnescah Shale (top at 80 ft deep) make up a packet of reflecting events within the Permian portion of the section that are easily identifiable and segregated on seismic sections. Bedrock is defined as the top of the Ninnescah Shale with the unconsolidated Plio-Pleistocene Equus Beds making up the majority of the upper 100 ft of sediment. Thickness of Quaternary alluvium that fills the stream valleys and paleo-subsidence features goes from 0 to as much as 300 ft thick depending on the particular features.

CMP Stacked Sections

CMP stacked sections from lines 1 and 2 fully image the target sinkhole at the intersection of Victory Road and U.S. 50 and unexpectedly several paleosinkholes with no current surface expression (Figures 15 and 16). Reflections above 200 ms possess a distinctive character and are within the primary interval of interest for delineating the geometry and failure mechanisms associated with the target subsidence feature.

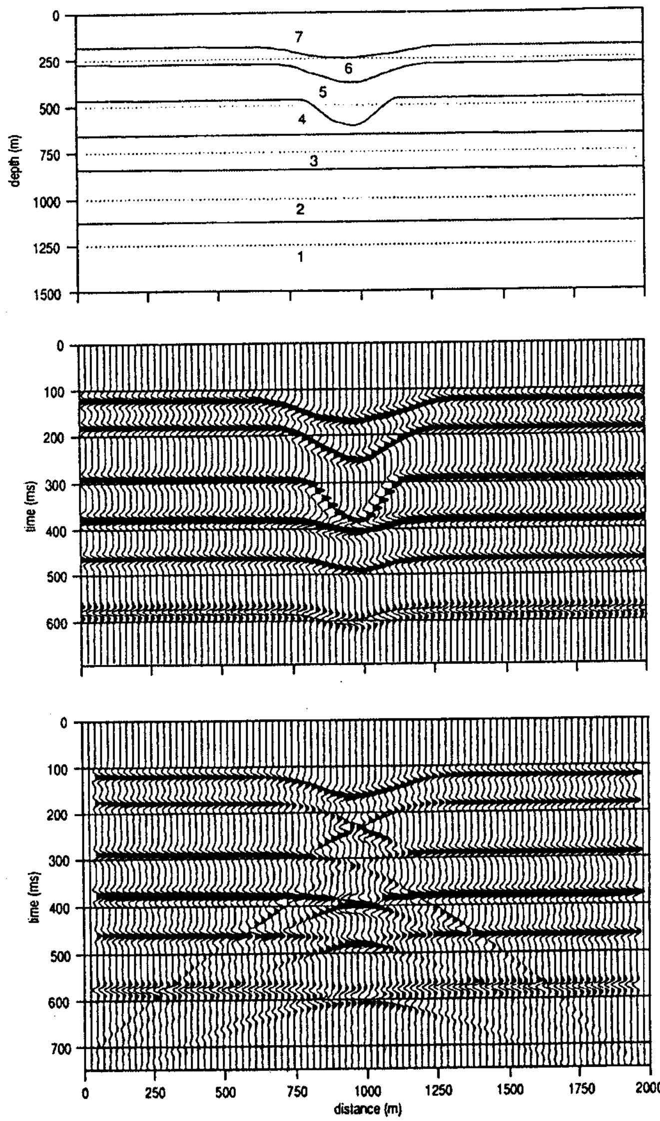

Figure 14. Geologic cross section of a simplified salt-dissolution feature and corresponding two-dimensional synthetic seismograms. The seismograms were generated from the geologic cross section, using 30 ms, zero-phase, normal-polarity Ricker wavelet, and vertical incidence and diffraction modeling techniques, respectively (from Anderson, 1995a).

High signal-to-noise ratio and bed resolution potential of reflections on shot and CMP gathers between depths of about 60 ft and 1000 ft suffer little degradation after horizontal stacking (Plates A and B). Bed resolution on the order of 5 to 15 ft, depending on reflection, was more than sufficient for confident delineation of rock layer geometries affected by the collapse of overburden into voids left after the leaching of the rock salt.

Migration was used to adjust for geometric distortion resulting from energy reflected from the tight synform that formed by rock layers subsiding into the voids left in the salt after dissolution (Figure 15b). With the NMO velocities in the Permian layers above 7000 ft/s and with the steeply dipping nature of the rock layers within the disturbed zone, it was necessary to migrate these data (Black et al., 1994). Migration clearly improves lateral coherency and the apparent signal-to-noise ratio and corrects for the distortion related to the moderate dip angle of the reflections, but at the price of slightly reduced resolution potential. The salt layer on migrated

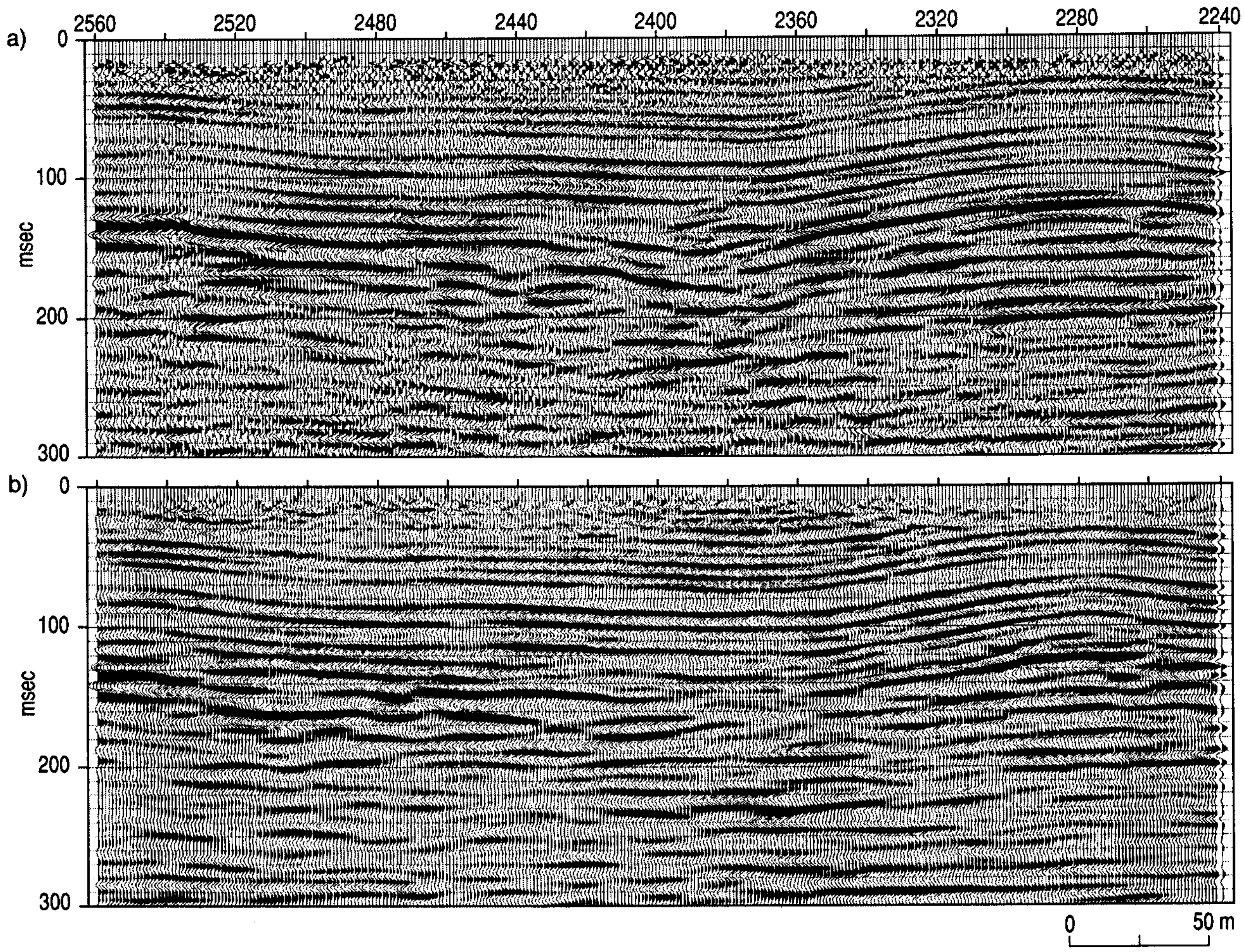

Figure 15. CMP stacked section of line 1. Bed distortion is exaggerated on this stacked section due in part to the decrease in average velocity within the disturbed portion of earth (a). The sinkhole is centered around station 2480. Migration corrected for much of the optical distortion that results from dipping beds, but reduced the resolution potential a bit (b). [Full migrated stacked section as Plate A.]

data is clearly defined by lower frequency and higher amplitude reflections. These higher amplitude reflections from within the salt interval itself are from laterally persistent thin anhydrite and shale layers interbedded with halite known to permeate the entire salt interval. The extreme undulations in reflections within the salt are not surprising considering both creep of the salt and associated subsidence of the inter-salt layers. Termination of the intra-salt reflections is likely related to the collapse of the less soluble anhydrite and shale units into voids left after dissolution of the salt. With the top of salt reflector clearly evident as the high amplitude reflection at about 130 ms, and the basal contact at about 180 ms, any bed irregularities below the salt are related to disturbances or nonlinearities in the wavefield that occur as energy travels through the shallower layers that have been disturbed by subsidence.

Seismic reflection data provides a clear image of the major rock units from bedrock (the top of the Ninnescah Shale), ranging in depth along this line from 70 to over 120 ft below ground surface (BGS), to significantly below the Permian/Pennsylvanian boundary at just over 1500 ft BGS (Plates C and D). The lowermost portion of the Equus Beds were imaged, but since the

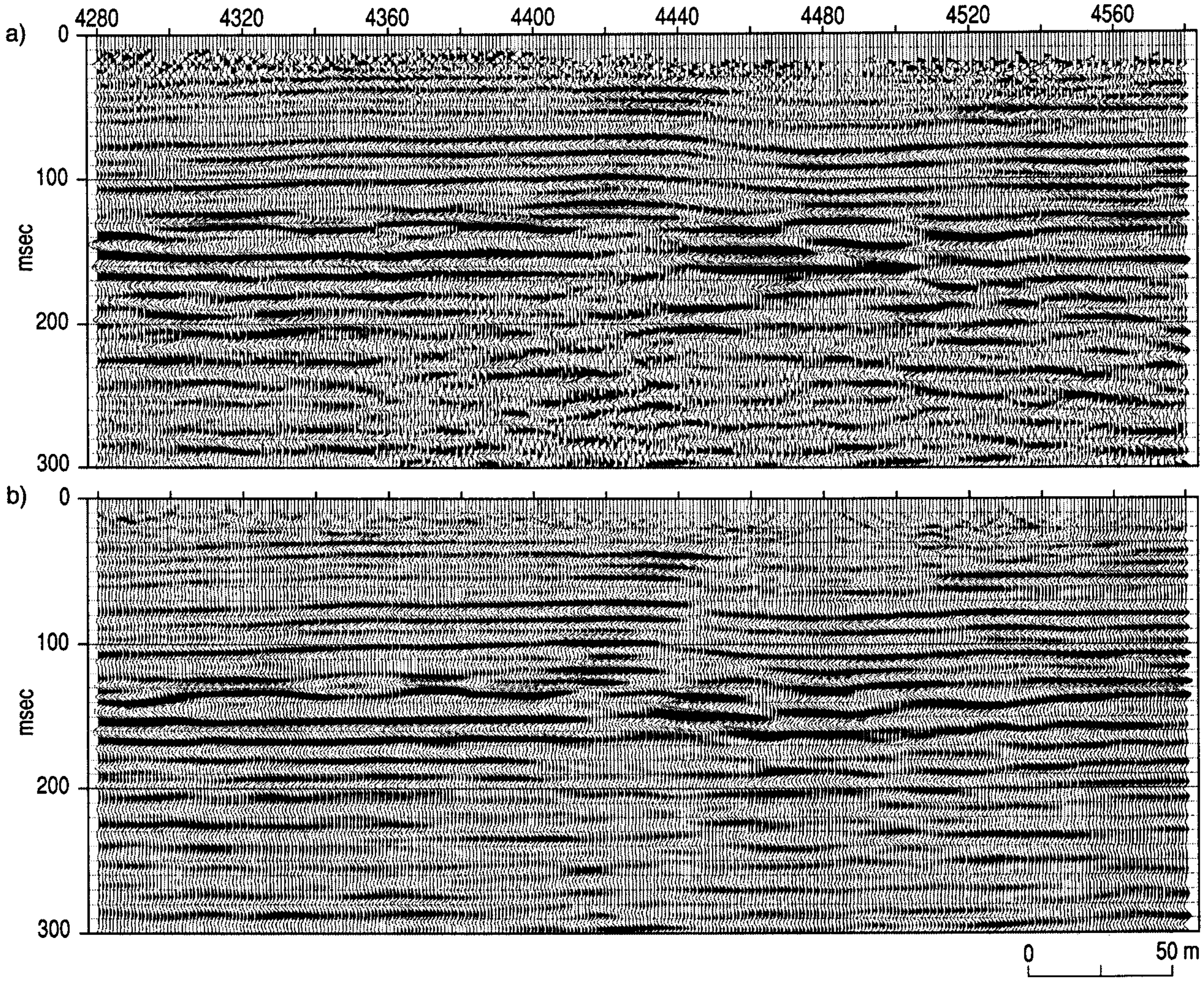

Figure 16. CMP stacked section of line 2. Bed distortion is exaggerated on this stacked section in part due to the decrease in average velocity within the disturbed portion of earth (a). The sinkhole is centered around station 4480. Migration corrected for much of the optical distortion that results from dipping beds, but reduced the resolution potential a bit (b). [Full migrated stacked section as Plate B.]

bedrock was the shallowest layer targeted during survey design, data were not recorded to optimally capture reflections from these water bearing unconsolidated sediments. Thickening and thinning of this unconfined, Plio-Pliestocene aquifer above current and paleo sinkholes provides clues to when subsidence has occurred in the past. In places the Equus Beds appear to fill the synform flatly in a fashion consistent with post-movement deposition. In other locations along these two lines these unconsolidated sediments seem to sag in a fashion generally consistent with the shale bedrock, implying movement was post-deposition. These observations suggest that some of these features were active as many as three different times in the last 65 million years: once during Tertiary and at least twice during Quaternary (including current active subsidence). Seismic arrivals associated with the bedrock, top and bottom of the Hutchinson Salt, and the Permian/Pennsylvanian boundary are all very distinct on CMP stacked sections and are easily correlated along each line and from line-to-line.

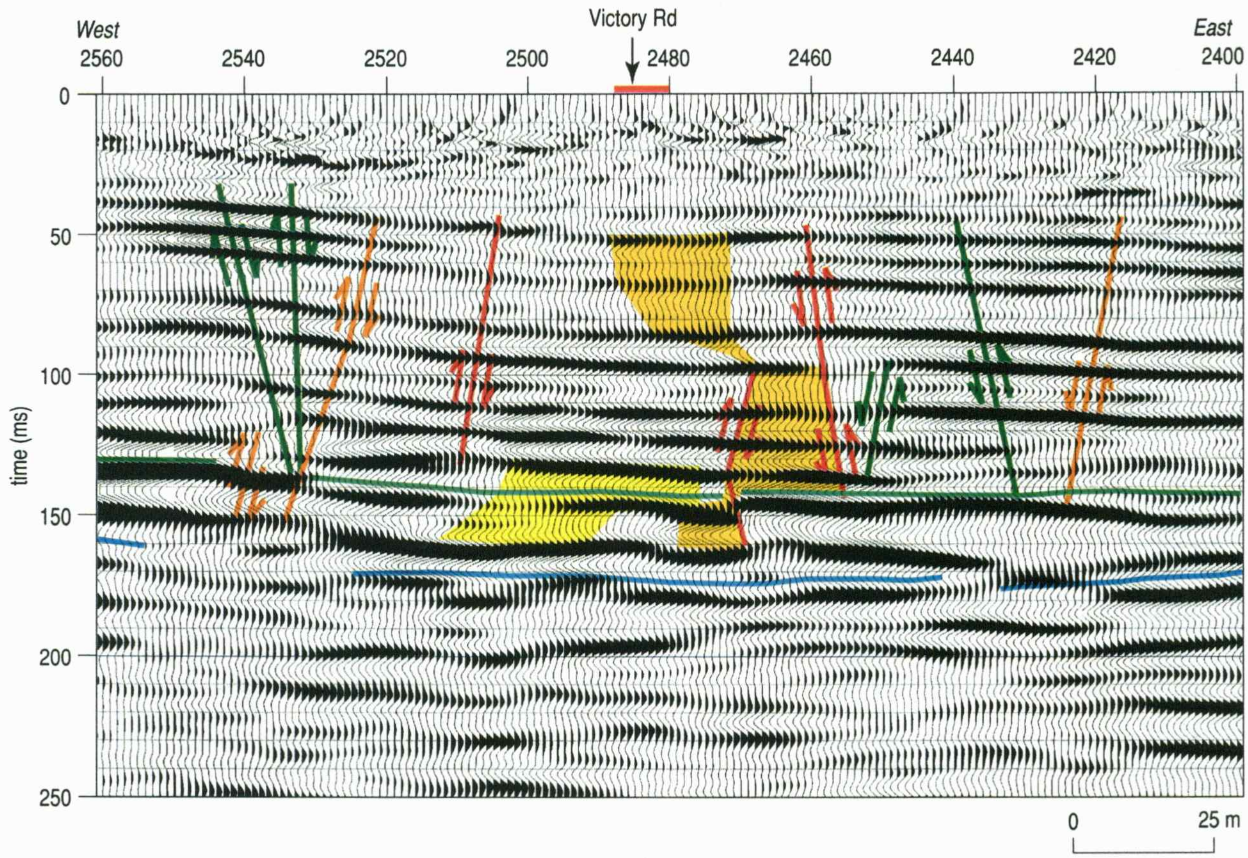

Figure 17. An interpreted portion of line 1 showing the original sinkhole margins as reverse oriented faults (gold) after rapid stress release in a brittle rupture fashion. This was followed by low velocity, low stress release forming a synform (bowl shaped depression) bounded by normal type faults (green). The most recent subsidence was again the result of rock failure and rapid stress release forming the tensional dome that beds subsiding along reverse fault plains (red). Orange shading represents areas currently active while yellow shading indicate areas for future concern.

Several episodes of subsidence are evident in most dissolution-related features (current and paleo) imaged on these two ¾-mile long seismic profiles (Plates E and F). Current surface subsidence at the intersection of U.S. 50 and Victory Road is probably related to the reactivation of natural salt dissolution processes, which produced the seismically imaged, 1500 ft wide subsidence feature. Focusing on the area likely active and currently associated with the sinkhole provides insight into present and recent processes (Figure 17). Paleosubsidences in and around the current sinkhole probably occurred at the very end of Tertiary or just prior to deposition of the Plio-Pleistocene Equus Beds. Dating this activity was to a large extent based on the appearance of subdued draping of the Equus Beds inside the deepest part of the bedrock low centered around station 2360. With this as the backdrop, a well-defined set of faults can be interpreted which likely define the formation of the paleosinkhole just northeast of the current sinkhole. The westernmost of these faults is about 150 ft from the current sinkhole. It appears that after the initial collapse, which defined the affected salt volume between about stations 2520 and 2380, came a period of gradual plastic deformation as the rock layers released stress, forming an evergrowing synform defined by faults with normal offset geometries.

The Permian bedrock surface varies in and around the subsidence features from 75 ft to as much as 150 ft below ground surface. The Equus Beds within the upper 40 ms clearly drape into bedrock lows formed from subsidence of Permian rocks over the main paleosinkhole along line 1 (Figure 17). Between the surface of bedrock and top of salt is a 125 ft thick sequence of red bed evaporites comprised mostly of shales. The very plastic nature of these shale units is evident in the conformal nature of the folding that overlies the highly altered beds of the salt unit. Amplitude changes across these folded units are interpreted in a very general sense as related to compaction, bridging, and energy scattering. Interpreting migrated data provided only minor improvement in differentiating the subsidence mechanisms and their sequence, but migration did focus much of the energy distortion associated with very localized (100 to 150 ft) undulations at the salt Upper Wellington contact (Figure 15b). Dramatic subsidence structures revealed on CMP stacked sections allude to a complex chronology of non-linear interaction between salt leaching and associated roof rock failure.

The boundary of the tensional dome is defined on the CMP stacked section by reverse faults (Figures 17 and 18). Faulting is interpreted to be coincident with a decrease in signal-to-noise ratio, apparent bed offset, and loss of coherency attributed to attenuation and scattering of energy along the planes (or in this case "zones") of failure. The beds between these reverse faults that define the tensional dome have undergone differing amounts of plastic and brittle deformation. This difference is attributed to differences in strength of the various lithologies and non-uniform leaching of the salt.

Using changes in amplitude and subtle breaks in rock layer slopes, the high angle reverse faults and subsidence cone (volume) can be defined (Plates E and F). A noticeable change in amplitude associated with drape in the bedrock beneath station 2480 on line 1 is interpreted to define the top of the subsidence cone. The subsidence volume appears, based on amplitude and geometry, to be nonsymmetrical, likely representative of the path of least strength. Faulting and differential compaction of materials within and above the salt represent a very unsettled earth defined by a variety of areas with layer bridging and the upward progression of subsidence. Apparent bridging above areas in the salt within the dissolution zone are good candidates for infilling by collapsing red bed sediments. With the volume of undercompacted earth (possibly void or rubble) suggested by the seismic section and proximity of the dissolution front, this area will continue to experience variable rates of subsidence significantly into the future.

A very subtle subsidence feature that appears to be completely separate from the present day sinkhole is either the beginnings of an aborted subsidence feature or a glimpse at a sinkhole in its early pre-development stage (Plate E). Formation of the characteristic synform or layer drape and inverted cone-like shape defined by reverse fault geometry seems to have halted at the contact between the Upper Wellington and Ninnescah shale units. This pause or halt might be an indication of the minimum length of roof span that can support the overburden materials in this area without initial failure. Most importantly, it might provide the quantifiable measure of the leach-out zone in salt necessary to begin the upward progression of a void toward the surface and formation of a sinkhole. Maybe even more importantly, this might be a critical find in helping designate catastrophic subsidence potential in and around facilities that require a stable earth. If the failure mechanism is consistent for this area, the angle of the fault planes and span of roof rock over the salt void will not be sufficient to reach the ground surface and form a sinkhole unless more salt is leached along the perimeter of this current salt void.

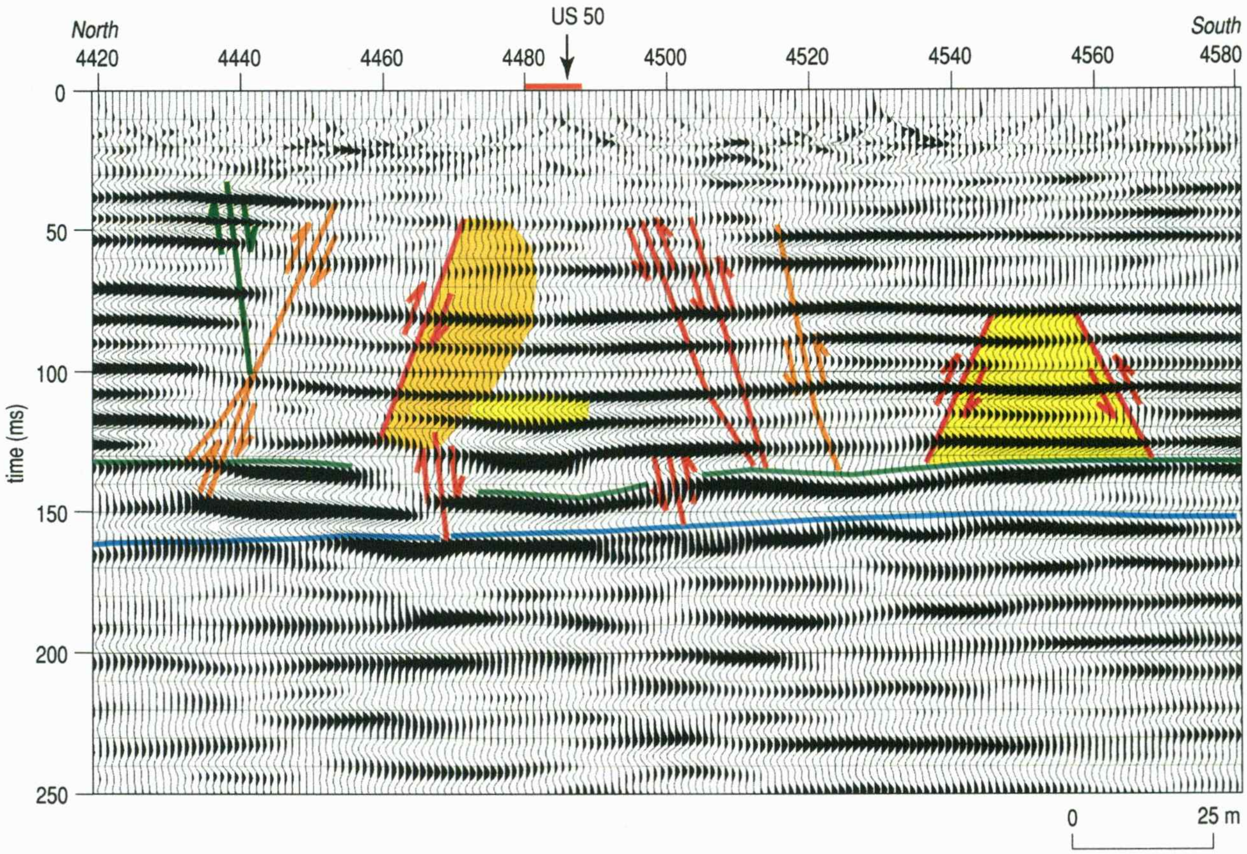

Figure 18. An interpreted portion of line 2 with the original sinkhole margins indicted by the reverse oriented faults (gold), which formed during rapid stress release during brittle rock failure. This was followed by low velocity, low stress release forming a synform (bowl-shaped depression) bounded by normal type faults (green). The most recent subsidence was again the result of rock failure and rapid stress release forming the tensional dome that beds subsiding along reverse fault plains (red). Yellow shading indicates areas for future concern.

Complexity and diversity of subsidence patterns along line 2 (Figure 18) are markedly different from that observed across line 1. The target sinkhole is for the most part symmetrically located within the subsurface subsidence zone and possesses a vertical expression consistent in size and geometry to subsidence features imaged on seismic data from sites where the dissolution catalyst was oil field brine leaking from injection wells. The subsidence feature at Victory Road and U.S. 50 appears to have a well-defined volume where salt has been or is being leached, allowing intra-salt anhydrite or shale units to drape and rupture along fault planes. Reverse faults define a cone of disturbed sediments associated with the original and most rapid subsidence areas at this site. Amplitude irregularities near the points of greatest offset in the redbed reflections mark the zones with the greatest distortion. This general area has experienced at least one period of gradual, low stress relief, indicated by the normal fault geometries. Consistent with line 1, the active cone of subsidence is bounded by reverse fault plains centered on the sinkhole.

The process responsible for the current sinkhole is not anomalous to rocks within this large paleostructure. It is probably one of many minor reactivations of dissolution and subsidence or roof rock failures associated with build-ups in stress that has gone on over hundreds of thousands of years. During times when stress was released at higher rates, material above the salt subsided along reverse fault plains. These fault planes define an ever-narrowing cone structure extending from the salt layer to the ground surface. Alternately, the current development of this sinkhole could be explained as recent failure of Permian rock layers above the salt previously bridging (roof rock) void or rubble areas that remained after the Tertiary to Quarternary subsidence that formed the paleosinkhole.

Paleostructures, such as those observed on these seismic data, clearly indicate natural dissolution processes have been at work here sometime, and probably several times, in the last million years or so. Pathways existed at some point in time (and may still exist today) that allowed fluid to gain access to the salt, harvest salt, and then transport that brine solution away from the salt dissolution front. Once this dissolution process produced a large enough void, the subsidence process began to breach the continuity of rock layers above the salt unit. This failure of rock layers within the tensional dome compromised the hydrologic confining characteristics of strata above the salt, creating more potential fluid pathways. The increase in fluid pathways to the salt could have easily increased the fluids available at the salt front to feed the leaching process and therefore accelerate the growth process and increase the aerial extent of the paleo-depression. Such a natural process would likely progress preferentially along natural trends defined by fractures, faults, or folds. Individual subsidence features and local swarms of subsidence features controlled by this type of natural process will be elongated along and aligned with the particular structure that provided the pathway for or guided fluids to access the dissolution front.

Active salt leaching in areas with pre-existing zones of structural weakness, such as paleosubsidence features, complicates this mechanical failure process and its predictability. Ruptured and distorted rock layers characterized on these seismic data as within paleosubsidence features would not likely possess the strength necessary to support the overburden across a long enough roof span for stress to build to a level of catastrophic failure potential (rapid formation of a sinkhole). For that reason alone, danger from catastrophic failure is greater where salt leaching is active and overlying rock layers are contiguous, with minimal to no drape (sag) and still possess their original/native strength properties (i.e., no paleosubsidence).

This leaching and subsidence process was active at the current sinkhole site at least twice: once when the current 300 ft wide sinkhole developed sometime in the past 10 years and prior to that when the 1500 ft wide dissolution feature (paleosinkhole) originally formed as a relatively continuous event (over a time frame of hundreds of thousands of years). The 1500 ft wide paleo-sinkhole footprint could be the result of dozens of uniquely segregated subsidence events occurring throughout the last million or so years. Each period of rapid subsidence was followed by a long period (not necessary represented by uniform or continuous rates) of slow downward movement (settling, relaxation) of sediments to release any accumulated stress outside the tensional dome that was left after initial failure of rock layers. These episodes of gradual subsidence advanced as the ever-expanding surface bowl structure, geometrically defined in the subsurface by normal fault planes. The rate of destabilization and failure as well as the load bearing potential of the rock layers above zones of dissolution strongly influenced both the original subsidence geometries and dimensions as well as the subsequent reactivation of subsidence along the profiles. At one time prior to the Quaternary infilling of this paleosinkhole it was over 50 ft deep and 1000 ft wide at the ground surface.

The current sinkhole expression and associated distortion of rock layers is the result of a minor episode of dissolution and subsidence in relation to the long history of dissolution and subsidence at this site. Rock layers along a span more than 1500 ft along line 1 have been altered by subsidence (Plate E and Figure 17). Changes in bed dip across this feature are key criteria for deciphering the sequence of dissolution and subsidence events that led to the current sinkhole. The north/south slice through the sinkhole provides a complementary but significantly different picture of the subsurface (Plate F and Figure 18). The root of the sinkhole along line 2 is only about 400 ft across and appears to have experienced two periods of activity. Both the individual features and gross structure of the subsidence along line 2 is consistent with dissolution failures interpreted previously that have formed after a breach in borehole confinement or overmining. Its structure does not rule out natural dissolution, but the line 2 feature alone more closely fits the anthropogenic model for the instigation of salt leaching. Coincident interpretation of lines 1 and 2 strongly support natural dissolution.

Mechanisms and gross chronology of structural failures as discernable from stacked seismic sections suggest initial subsidence and associated bed offset at this site occurred "rapidly" as accumulated stress was released (Figures 17 and 18). Bed offset during the initial as well as intermediate growth stages was constrained to the tensional dome. The tensional dome for this sinkhole reached the ground surface during the later stages of development and therefore the surface subsidence occurred over years rather than days or minutes. Current growth appears to be along normal fault planes and is therefore associated with relaxation of stress in rocks outside the tensional dome and will proceed at a gradual and slowing rate. This slow down assumes no more salt is or will be leached from beneath this sinkhole in association with this subsidence event.

Conclusions

Five unique dissolution features were imaged and interpreted during this study (Figure 19). First and foremost was the subsurface expression of the sinkhole at the intersection of U.S. 50 and Victory Road in Reno County, Kansas. Associated with the active subsidence feature is the paleosinkhole elongated in an east/west direction with a long axis of over 1500 ft. The geometry of both subsurface structures associated with the current sinkhole are quite similar, likely a key indication that fluid pathways and transport mechanism are the same for both. Two other paleosubidence features were identified with some indication that rock layers outside the tensional dome might still have stress build-up associated with bridging. Maybe the most speculative feature is the small subsidence cone observed near station 2800 on the east/west line, suggested to be part of the root of a future sinkhole in a very preliminary stage of development. Several areas along U.S. 50 have dissolution features present that justify monitoring.

Apparent undulations in the surface of the Hutchinson Salt layer could be indicative of dissolution features bridged by undisturbed rock layers with a span not yet sufficient for the accumulated load to instigate roof failure. Roof rock failure above these voids can proceed at varying rates and affect different portions of the overlying rock column. These undulations could also be indicative of changes in water chemistry (salinity) during or near the conclusion of salt deposition in this area. An apparent halt in the upward movement of a dissolution feature (downward movement of sediments) at the boundary between the Ninnescah Shale and the

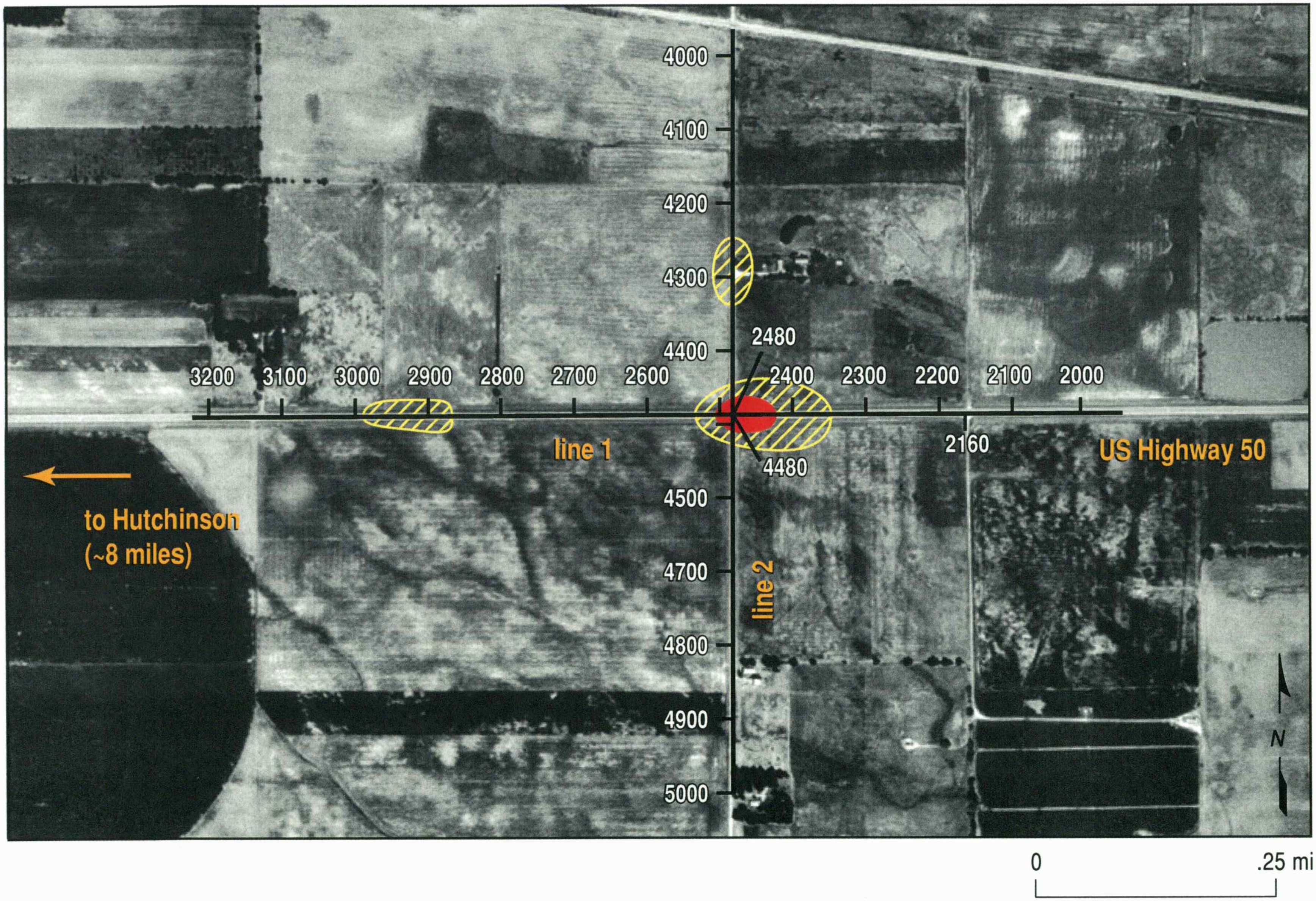

Figure 19. Station locations and key dissolution features interpreted on seismic data.

Upper Wellington Shale could be a key indicator as to the effective unsupported span of roof rock these shallow shale layers can support.

Interpretation of reflections from key stratigraphic horizons suggest plastic deformation of rock layers over dissolution voids was followed by roof rock failure along reverse fault planes within an earth volume known as the tension dome. The original tensional dome was centered on the dissolution volume and extended from the base of the salt interval to near the surface. A long period of relaxation of stress associated with layers outside the tensional dome occurred along normal fault planes for a significant portion of the late Tertiary and early Quaternary. A much smaller tensional dome located at the western extreme of the original tensional dome controls current subsidence at this site. Subsidence associated with failure defined by this most recent dome has followed a somewhat asymmetric path from salt to surface.

With a subsidence history at this site potentially extending as far back as mid-Tertiary, it is unlikely subsidence will end within the next millennium. Until the highway started sinking at this location during 1998, little if any subsidence seems to have been associated with this paleosinkhole throughout late Quaternary. This long period of inactivity followed by the localized, rapid subsidence observed at this site suggests that other small sinkholes could form without warning above this paleofeature or other similar paleofeatures in this area. Considering the interpreted bed geometries, surface subsidence at the current sinkhole site will likely continue gradually along its northern and eastern edges, elongating the sinkhole in those directions. Besides the obvious disruption to the road system, unfortunately this subsidence feature provides a pathway between the fresh waters of the Equus Beds and the more brackish waters of the Permian. Surface subsidence will likely continue at a gradual rate for some time into the future. Sufficient bridging and undercompacted rock layers still exist beneath this sinkhole to sustain the current subsidence rate of around 1 ft/yr for several years.

Acknowledgements

The author would like to thank Mike Dealy from GMD2 and Morris Korphage and Doug Lewis from the KCC for their support of this project. Rex Buchanan at the Kansas Geological Survey provided assistance with lighting during media coverage and was cheerer for the crew. Thanks also to the field crew: David Laflen, Joe Anderson, Mitchell Fiedler, and Chad Gratton. As always, the assistance of Brett Bennett and Mary Brohammer during field and report preparations is appreciated.

References

Anderson, N.L., W.L. Watney, P.A. Macfarlane, and R.W. Knapp, 1995a, Seismic signature of the Hutchinson Salt and associated dissolution features: Kansas Geol. Survey Bulletin 237, p. 57-65.

Anderson, N.L., R.W. Knapp, D.W. Steeples, and R.D. Miller, 1995b, Plastic deformation and dissolution of the Hutchinson Salt Member in Kansas: Kansas Geol. Survey Bulletin 237, p. 66-70.

Anderson, N.L., A. Martinez, and J.F. Hopkins, 1998, Salt dissolution and surface subsidence in central Kansas: A seismic investigation of the anthropogenic and natural origin models: Geophysics, v. 63, p. 366-378.

Baar, C.A., 1977, Applied salt-rock Mechanics 1: Elsevier Scientific Publishing Company, 294 p.

Baker, G.S., D.W. Steeples, and M. Drake, 1998, Muting the noise cone in near-surface reflection data: An example from southeastern Kansas: Geophysics, v. 63, p. 1332-1338.

Bayne, C.K., 1956, Geology and ground-water resources of Reno County, Kansas: Kansas Geological Survey Bulletin 120.

Beck, B.F., A.J. Pettit, and J.G. Herring, eds., 1999, Hydrogeology and engineering geology of sinkholes and Karst–1999: A.A. Balkema.

Black, R.A., D.W. Steeples, and R.D. Miller, 1994, Migration of shallow seismic reflection data: Geophysics, v. 59, p. 402-410.

Carter, N.L., and F.D. Hansen, 1983, Creep of rock salt: Tectonophysics, v. 92, p. 275-333.

Doll, W.E., and C. Çoruh, 1995, Spectral whitening of impulsive and swept-source shallow seismic data [Exp. Abs.]: Soc. Explor. Geophys., p. 398-401.

Davies, W.E., 1951, Mechanics of cavern breakdown: National Speleological Society, v. 13, p. 6-43.

Ege, J.R., 1984, Formation of solution-subsidence sinkholes above salt beds: U.S. Geological Survey Circular 897, 11 p.

Frye, J.C., 1950, Origin of Kansas Great Plains depressions: Kansas Geological Survey Bulletin 86, pt. 1, p. 1-20.

Frye, J.C., and S.L. Schoff, 1942, Deep-seated solution in the Meade Basin and vicinity, Kansas and Oklahoma: American Geophysical Union Transactions, v. 23, pt. 1, p. 35-39.

Hunter, J.A., S.E. Pullan, R.A. Burns, R.M. Gagne, and R.S. Good, 1984, Shallow seismic-reflection mapping of the overburden-bedrock interface with the engineering seismograph–Some simple techniques: Geophysics, v. 49, p. 1381-1385.

Knapp, R.W., D.W. Steeples, R.D. Miller, and C.D. McElwee, 1989, Seismic reflection surveys at sinkholes in central Kansas: Geophysics in Kansas, D.W Steeples, ed.: Kansas Geological Survey Bulletin 226, p. 95-116.

Liberty, L.M., and M. Knoll, 1998, Time varying fold in high-resolution seismic reflection data: a recipe for optimized acquisition and quality control processing and interpretation: Proceedings of the Symposium on the Application of Geophysics to Engineering and Environmental Problems (SAGEEP 98), March 22-26, Chicago, p. 745-751.

Merriam, D.F., and C.J. Mann, 1957, Sinkholes and related geologic features in Kansas: Transactions Kansas Academy of Science, v. 60, p. 207-243.

Merriam, D.F., 1963, The geologic history of Kansas: Kansas Geol. Survey Bulletin 162, 317 p.

Miller, R.D., D.W. Steeples, L. Schulte, and J. Davenport, 1993, Shallow seismic reflection study of a salt dissolution well field near Hutchinson, Kansas: Mining Engineering, October, p. 1291-1296.

Miller, R.D., D.W. Steeples, and J.A. Treadway, 1985, Seismic reflection survey of a sinkhole in Ellsworth County, Kansas [Exp. Abs.]: Soc. Explor. Geophys. 55th Ann. Mtg., Washington, D.C., p. 154-156.

Miller, R.D., D.W. Steeples, and T.V. Weis, 1995, Shallow seismic-reflection study of a salt-dissolution subsidence feature in Stafford County, Kansas: in N.L. Anderson and D.E. Hedke, eds., Geophysical Atlas of Selected Oil and Gas Fields in Kansas: Kansas Geological Survey Bulletin 237, p. 71-76.

Miller, R.D., A.C. Villella, J. Xia, 1997, Shallow high-resolution seismic reflection to delineate upper 400 m around a collapse feature in central Kansas: Environmental Geosciences, v. 4, n. 3, p. 119-126.

Rokar, R.B., and K. Staudtmeister, 1985, Creep rupture criteria for rock salt: Sixth International Symposium on Salt, B.C. Schreiber and H.L. Harner, eds., Salt Institute Inc., Virginia, v. 1, p. 455-462.

Steeples, D.W., R.W. Knapp, and C.D. McElwee, 1986, Seismic reflection investigation of sinkholes beneath interstate highway 70 in Kansas: Geophysics, v. 51, p. 295-301.

Steeples, D.W., and Miller, R.D., 1990, Seismic reflection methods applied to engineering, environmental, and groundwater problems: Soc. Explor. Geophys., Geotechnical and Environmental Geophysics, Stan Ward, ed., Vol. 1: Review and tutorial, p. 1-30.

Walters, R.F., 1978, Land subsidence in central Kansas related to salt dissolution: Kansas Geological Survey Bulletin 214, p. 1-32.
Walters, R.F., 1980, Solution and collapse features in the salt near Hutchinson, Kansas: South-central Section, Geological Society of America, Field Trip Notes, 10 p.
Walters, R.F., 1991, Gorham Oil Field: Kansas Geological Survey Bulletin 228, p. 1-112.
Watney, W.L., J.A. Berg, and S. Paul, 1988, Origin and distribution of the Hutchinson Salt (lower Leonardian) in Kansas: Midcontinent SEPM Special Publication No. 1., p. 113-135.
Xia and Miller, 2000, Design of a hum filter for suppressing power-line noise in seismic data: Journal of Environmental and Engineering Geophysics, v. 5, n. 2, p. 31-38.

Fig A7. Looking generally west across sinkhole north of intersection of U.S. 50 and Victory Road.

Fig A8. Winding cable along east road ditch of Victory Road south of U.S. 50.

Fig A9. Geophones collected on a metal hasp designed to carry as many as 12 strings.

Fig A10. Looking north on Victory Road toward U.S. 50 as tractor trailer enters into sinkhole.

Fig A11. Seismograph vehicle along Victory Road south of U.S. 50.

Fig A12. Cable, phones, and support tubs along line 2 on Victory Road.

Appendix B
PowerPoint Presentation on U.S. 50 Sinkhole Study

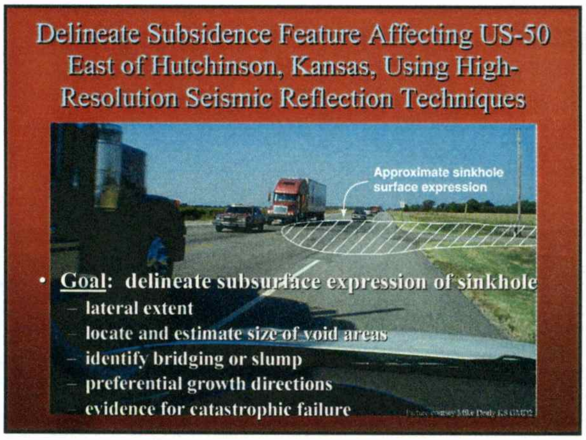

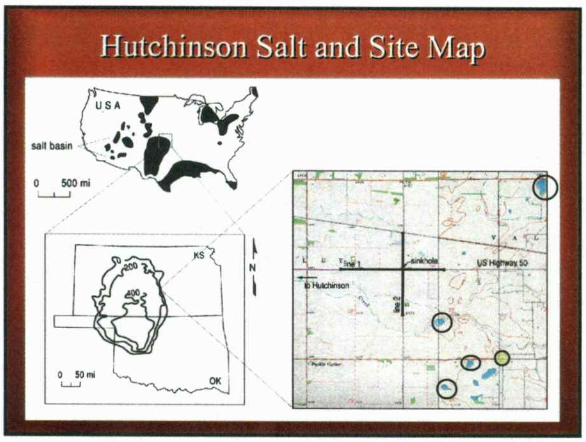

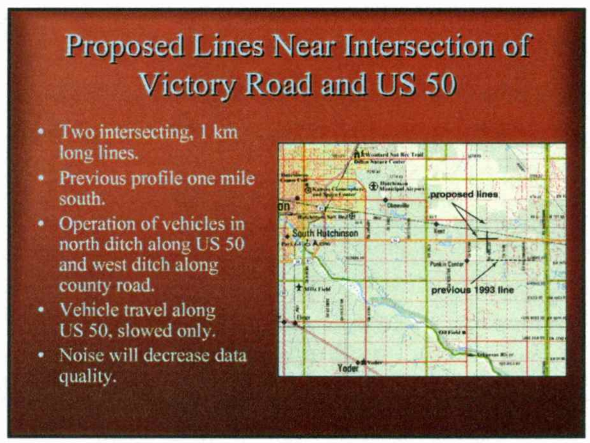

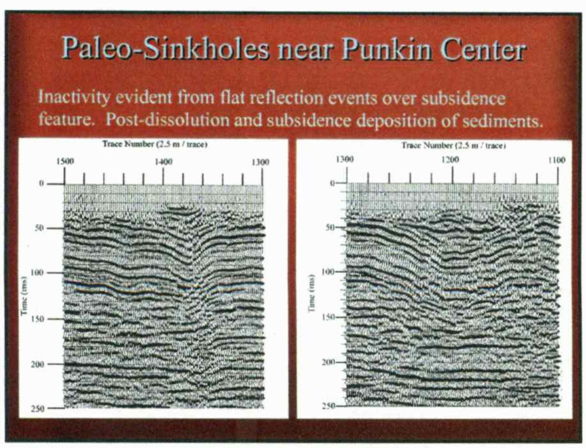

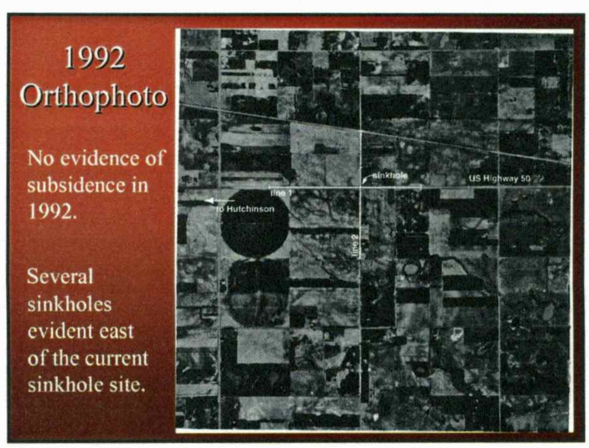


Acquisition Equipment

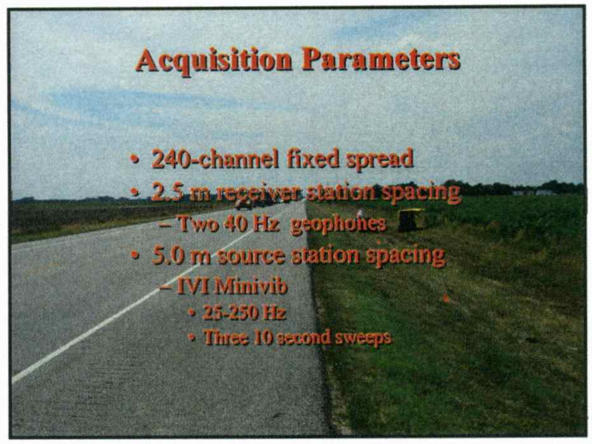
Acquisition Parameters
• 240-channel fixed spread
• 2.5 m receiver station spacing
– Two 40 Hz geophones
• 5.0 m source station spacing
– IVI Minivib
• 25-250 Hz
• Three 10 second sweeps


Test data conclusively demonstrated that receivers in base of ditch and source on road shoulder were optimum for this site.

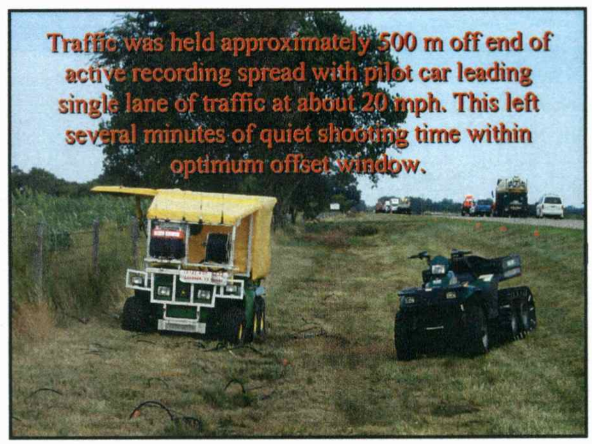
Traffic was held approximately 500 m off end of active recording spread with pilot car leading single lane of traffic at about 20 mph. This left several minutes of quiet shooting time within optimum offset window.


A 240-channel fixed spread allowed the recording unit to remain stationary while the source traversed about 600 m of line and recorded fully within the optimum offset window without a roll-along box.

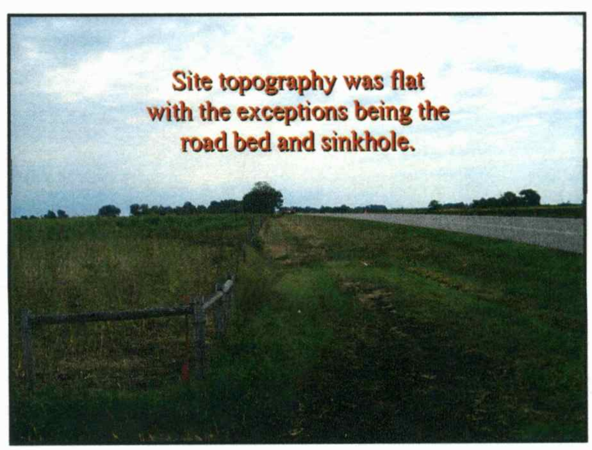
Site topography was flat with the exceptions being the road bed and sinkhole.

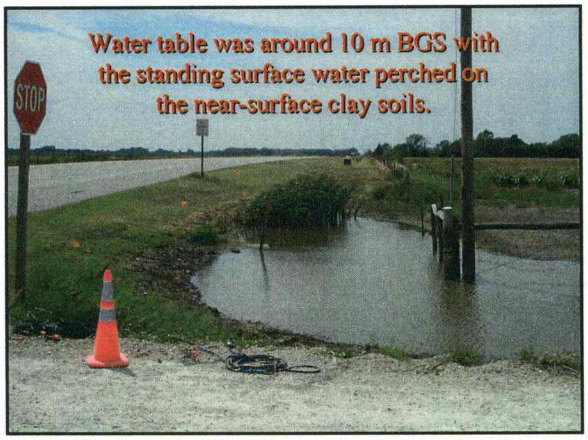
Water table was around 10 m BGS with
the standing surface water perched on
the near-surface clay soils.
STOP

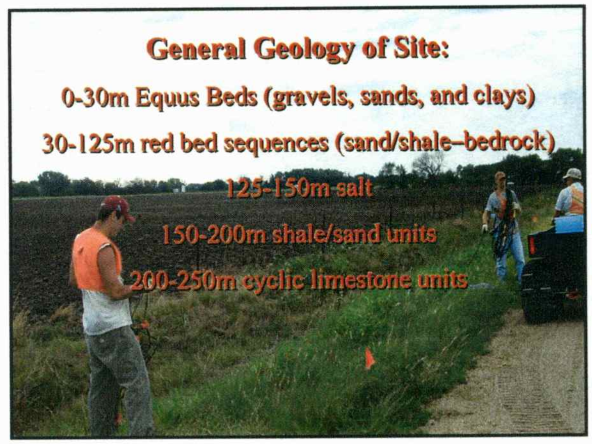
General Geology of Site:
0-30m Equus Beds (gravels, sands, and clays)
30-125m red bed sequences (sand/shale–bedrock)
125-150m salt
150-200m shale/sand units
200-250m cyclic limestone units

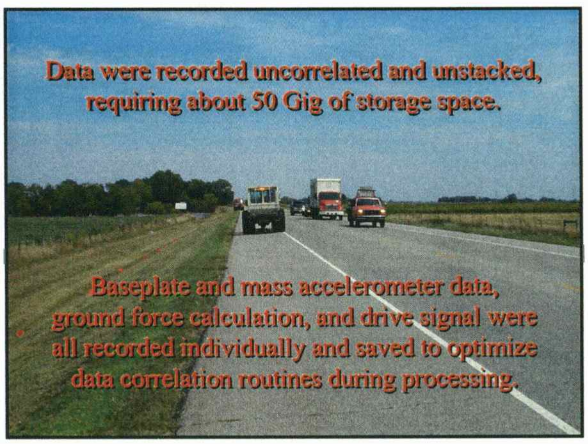
Data were recorded uncorrelated and unstacked,
requiring about 50 Gig of storage space.
Baseplate and mass accelerometer data,
ground force calculation, and drive signal were
all recorded individually and saved to optimize
data correlation routines during processing.


A 5 m source spacing best matched data
quality (fold and offsets) with survey
economics.

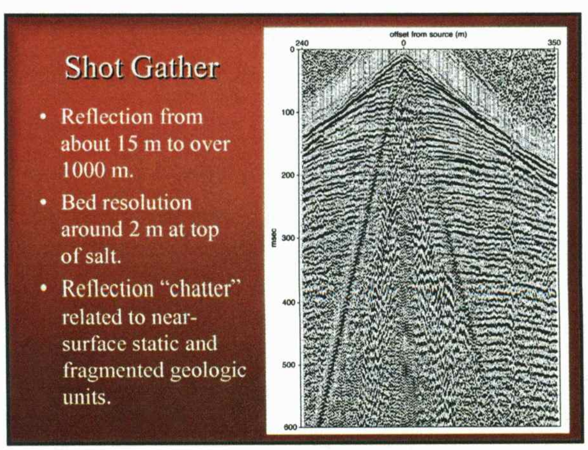
Shot Gather
• Reflection from about 15 m to over 1000 m.
• Bed resolution around 2 m at top of salt.
• Reflection "chatter" related to near-surface static and fragmented geologic units.
offset from source (m)
240
0
350
msec
100
200
300
400
500
600

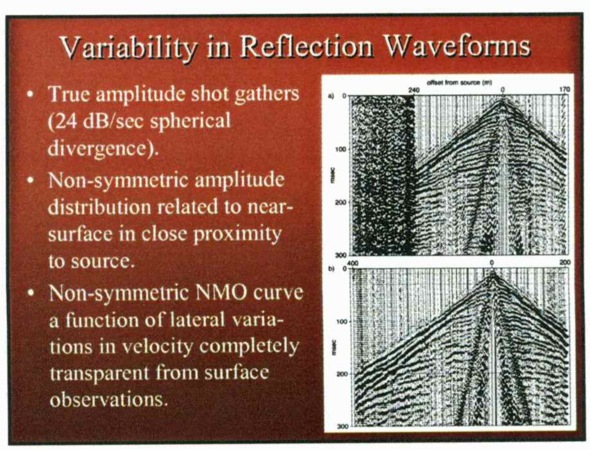
Variability in Reflection Waveforms
• True amplitude shot gathers (24 dB/sec spherical divergence).
• Non-symmetric amplitude distribution related to near-surface in close proximity to source.
• Non-symmetric NMO curve a function of lateral variations in velocity completely transparent from surface observations.
offset from source (m)

Ultra-Shallow Reflections

- Events less than 30 ms on stacked sections need to be confidently identified on shot gathers.
- Clear indications of disturbed subsurface evident on shot gathers.
- 10 ms time arrival difference on opposite sides of the source.

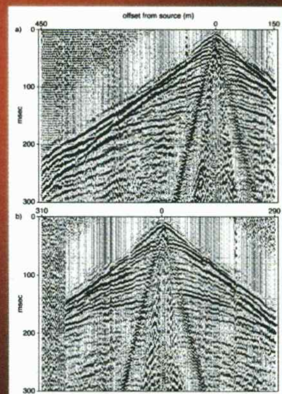

Processed CMP Gather

- Pre-correlation AGC scale 1 sec
- Hum filter (power line noise)
- Spherical diverg.
- Aggressive mute: inside, top, noise
- NMO stretch <13%
- Surface consistent statics (3 iterations)
- F-k migration

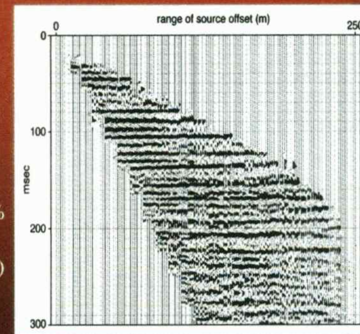

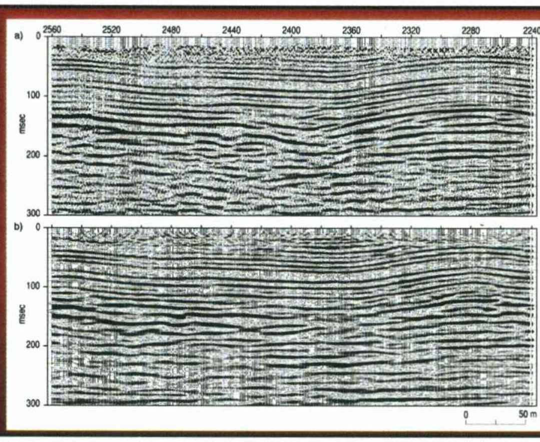

Migration: Correct for Optical Distortion

- Severity of "bowl" or synform from subsidence affects diffracted energy.
- Apparent extension of layer into subsidence zone, horizontal resolution limitation.
- Subsidence layers above salt alter velocity and result in apparent drop in layers below salt.

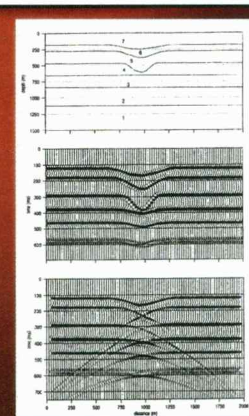

Modified from Anderson et al 1995

Interpretation of West/East Profile

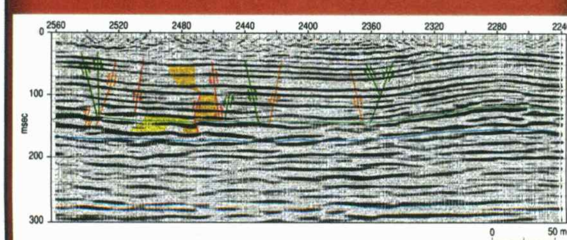

- Several episodes of subsidence
- Characterized by both normal and reverse type faults
- Bridging and undercompacted (relative) materials

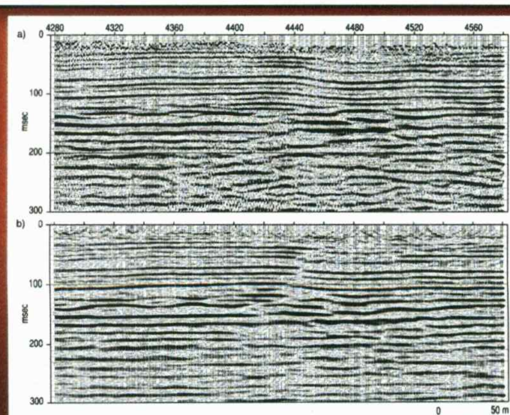

Interpreted North/South Profile

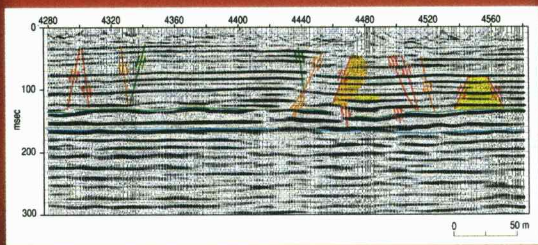

- Constrained to small fault-defined area
- Aborted subsidence feature
- Dormant paleosinkhole

- Stress lines and flexure prior to roof failure.
- Rock properties and formation geometry dictate failure rate.
- Reverse faults initially, with normal faults associated with gradual subsidence.

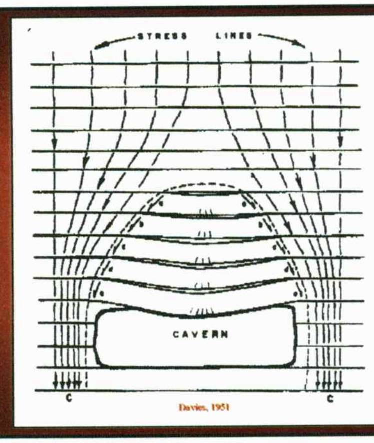

French Sinkhole west of St. John in Stafford, Kansas

- KCC investigation of subsidence potential and failure rate to evaluate risk to plugging crew.
- Two surveys look at change.

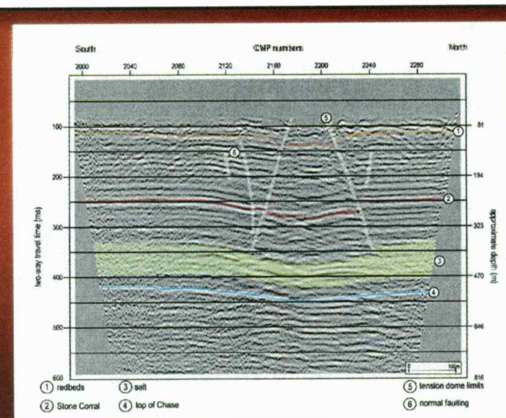

Active Subsidence Area W/E Line

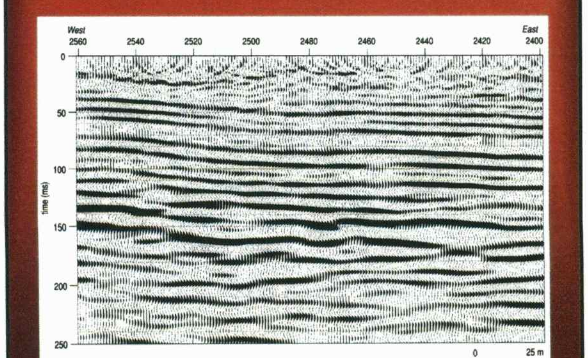

Interpreted W/E Active Section

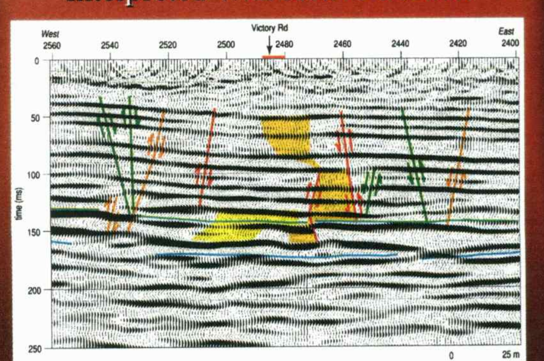

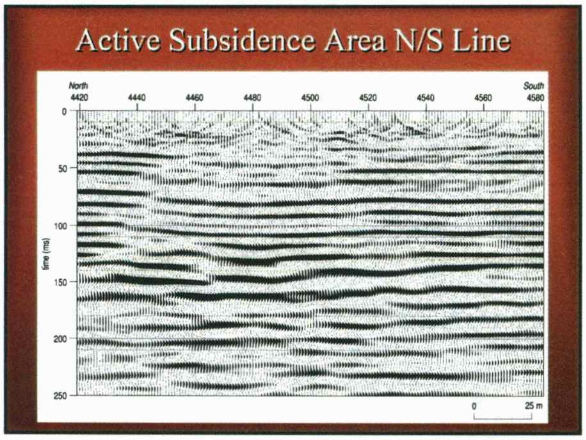
Active Subsidence Area N/S Line
North
South
4420 4440 4460 4480 4500 4520 4540 4560 4580
time (ms)
0 50 100 150 200 250
0 25 m

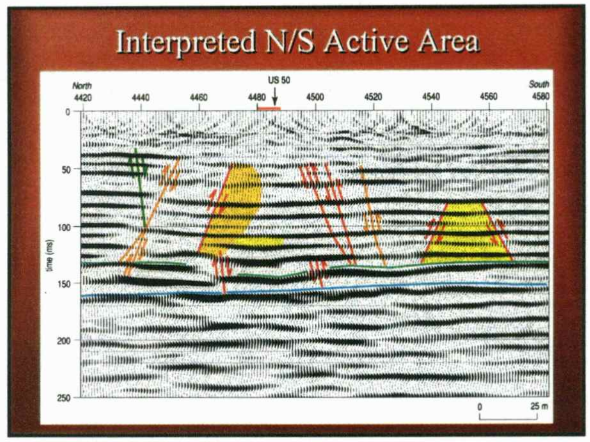
Interpreted N/S Active Area
US 50
North
South
4420 4440 4460 4480 4500 4520 4540 4560 4580
time (ms)
0 50 100 150 200 250
0 25 m

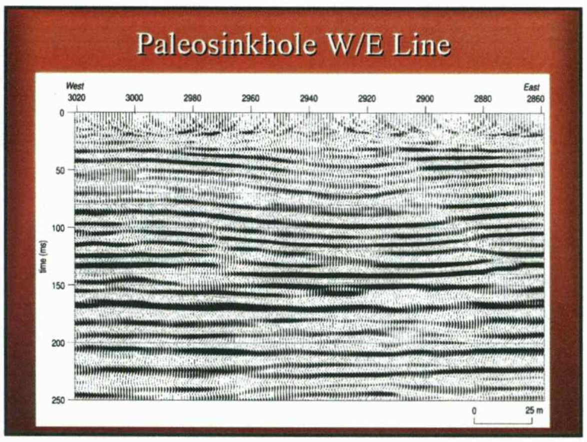
Paleosinkhole W/E Line
West
East
3020 3000 2980 2960 2940 2920 2900 2880 2860
time (ms)
0 50 100 150 200 250
0 25 m

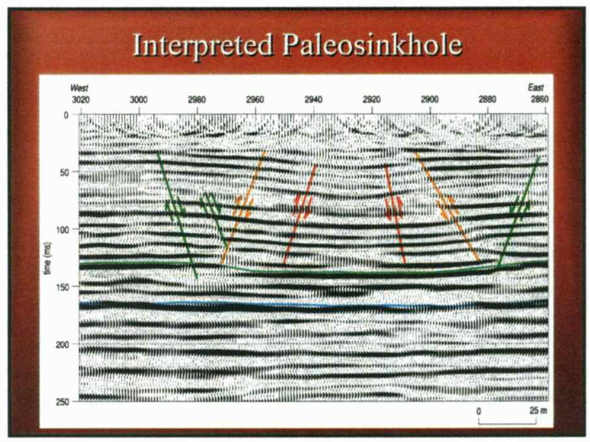
Interpreted Paleosinkhole
West
East
3020 3000 2980 2960 2940 2920 2900 2880 2860
time (ms)
0 50 100 150 200 250
0 25 m

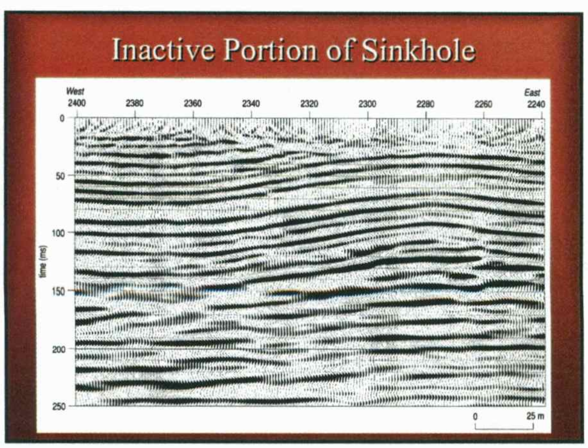
Inactive Portion of Sinkhole
West
East
2400 2380 2360 2340 2320 2300 2280 2260 2240
time (ms)
0 50 100 150 200 250
0 25 m

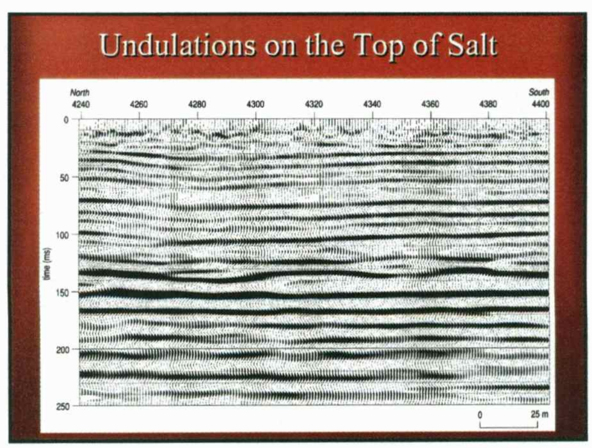
Undulations on the Top of Salt
North
South
4240 4260 4280 4300 4320 4340 4360 4380 4400
time (ms)
0 50 100 150 200 250
0 25 m

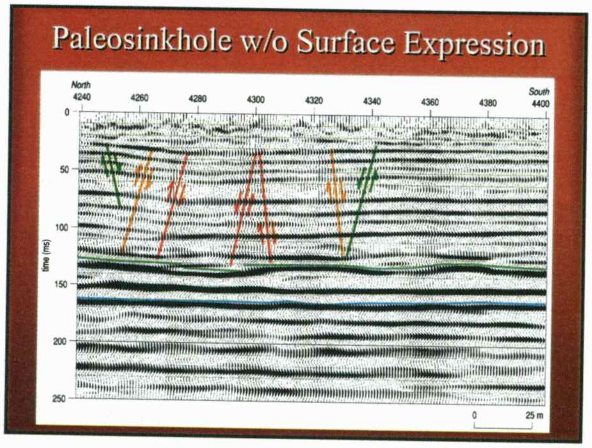
Paleosinkhole w/o Surface Expression
North
South
4240
4260
4280
4300
4320
4340
4360
4380
4400
time (ms)
0
50
100
150
200
250
0
25 m

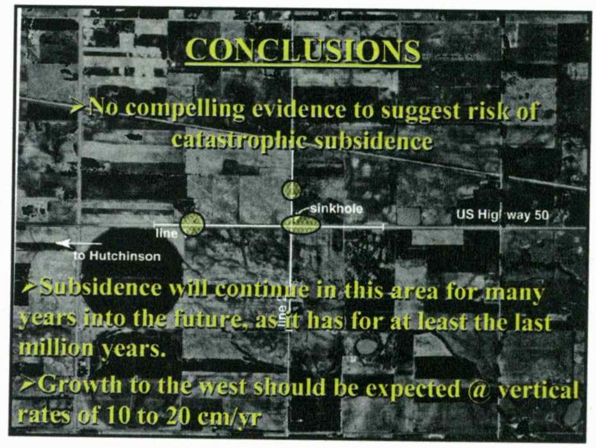
CONCLUSIONS
➢No compelling evidence to suggest risk of catastrophic subsidence
sinkhole
US Highway 50
line
to Hutchinson
line
➢Subsidence will continue in this area for many years into the future, as it has for at least the last million years.
➢Growth to the west should be expected @ vertical rates of 10 to 20 cm/yr

Appendix C
PowerPoint Presentation on the Seismic Reflection Concept and Technique

Elastic Waves Travel Paths

- Layer over half-space
- Energy partitioning dependent on angle of incidence and velocity/density contrast
- Identify by unique arrival pattern and apparent phase velocity
- Surface wave (ocean wave)
  - Love wave
  - Rayleigh wave
- Body wave (rays)
  - P-waves (compressional)
  - S-Waves (shear)

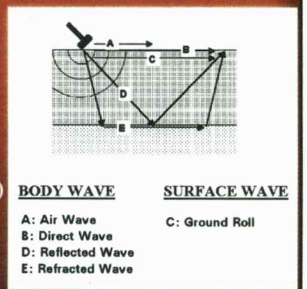

Seismic Velocities

- Compressional

  $V_P = \{(\lambda + 2\mu)/\rho\}^{1/2}$
- Shear

  $V_S = (\mu/\rho)^{1/2}$
- Surface (dispersive)
  - Rayleigh

    $V_R = 0.92\ V_S\ (V_P, V_S, z, \rho)$
  - Love

    $V_L = \sim 0.9\ V_S$

Reflectivity

- Snell's Law at Interface
  - reflected
  - refracted
  - transmitted

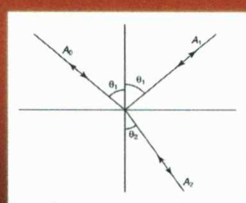

Reflection Concept: Geologic Model

- Sands/silts/gravels with lenticular clays acting as confining units
- Objective: image top and bottom of clay lens
- Potential for determining depth and layer thickness dependent on velocity and frequency

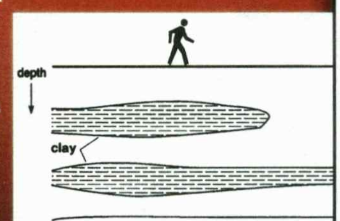

Reflection Concept: Seismic Raypaths

- Energy source detonates, impacts, or transmits wavetrain
- Seismic waves travel in all directions from the source, reflecting from layers with a velocity and/or density contrast
- Reflected energy arrives at the receivers along travel paths consistent with source offset and depth to reflector and at times related to average material velocities the energy traveled through

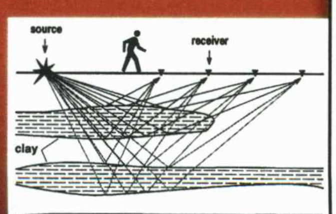

Reflection Concept: Arrival Pattern

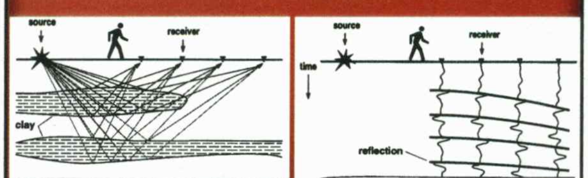

Energy arrivals returning from subsurface layers are measured in time. The arrival pattern of energy pulses reflected from subsurface layers possesses a hyperbolic curvature (Normal Move Out–NMO). This curvature is diagnostic of reflections and has a shape dictated by the velocity of materials above the reflecting interface.

Unique Velocity Curvature

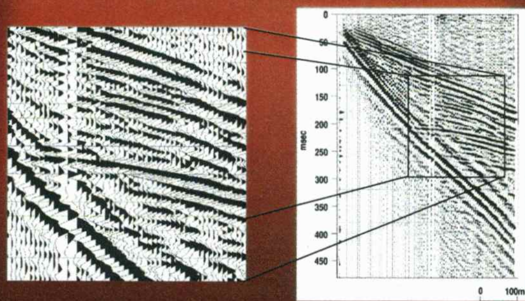

Reflection Concept: Correct for Offset

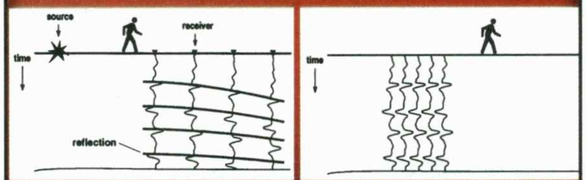

Arrival times of reflection events are adjusted for offset. This process places all reflections at a time representative of zero offset from the source. By making this adjustment traces can be horizontally stacked to enhance signal at the expense of noise. Due to the curved nature of the arrivals (NMO) the time adjustment necessary to simulate vertical incidence is non-linear with offset and depth.

Reflection Concept: Interpretation

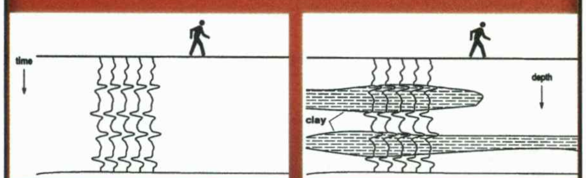

Arrival times of reflection events must be correctly adjusted for offset. This processes, based on the NMO velocity, places all reflections at times representative of zero source offset. This adjustment allows horizontal stacking of traces to enhance signal at the expense of noise. The time adjustment of each trace necessary to simulate vertical incidence is non-linear with offset and depth.

Common Mid Point (CMP)

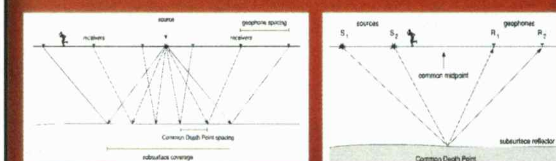

- With multiple receivers recording for a single shot the subsurface can be sampled once for each receiver.
- Resolution, related to frequency, determines how small a layer or object we can image.
- Each subsurface point will be imaged several times (fold).
- Moving source and receivers provides continuous coverage.

Seismic Reflection Imaging

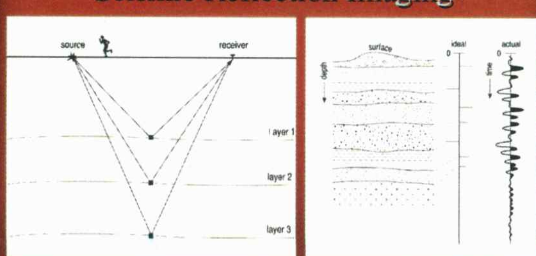

Energy from a seismic source echoes (reflects) from rock layers producing unique energy burst (wiggles) which return to the earth's surface where receivers (geophones) listen and convert these echoes into electric voltages as a function of time relative to when the energy left the source. Time from source to receiver is converted to depth.

Interpretation

⇒ Interpretation starts with the shot gather

⇒ Modeling at all stages of acquisition and processing

⇒ Follow coherent events throughout processing flow

⇒ Every wiggle or attribute change does not have a unique geologic significance

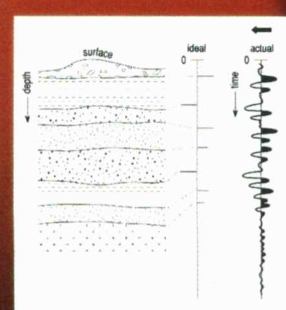

Resolution Directly Related to Frequency and Velocity

Detecting presence of void and collapse features in the shallow subsurface

Delineating objects and structures in the shallow subsurface

Migration: Correct for Optical Distortion

- Severity of "bowl" or synform from subsidence effects diffracted energy
- Apparent extension of layer into subsidence zone, horizontal resolution limitation
- Subsidence layers above salt alter velocity and result in apparent drap in layers below salt

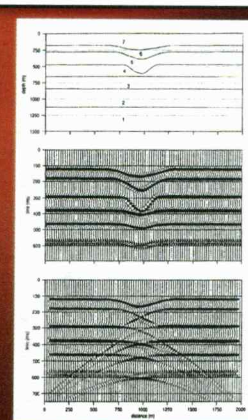

Appendix A
Field Photographs, August 21-24, 2001

Fig A1. Seismograph mounted in John Deere Gator along seismic line 1 with tracked 6-wheel-drive Polaris cable/phone vehicle.

Fig A2. Vibrator along north road shoulder with KDOT pilot car managing traffic on U.S. 50.

Fig A3. Sinkhole at the northwest corner of the intersection of Victory Road and U.S. 50 in Reno County.

Fig A4. Seismograph vehicle with cables and phones in ditch and KDOT pilot car in the background.

Fig A5. Vibrator along westbound shoulder of U.S. 50.

Fig A6. Road ditch looking northeast from sinkhole with U.S. 50 along south side of line.